R.C. Figueiredo e Silva et al. / Geonomos, 19(2), 198-223, 2011
www.igc.ufmg.br/geonomos

Petrographic and geochemical studies at giant Serra Norte iron ore deposits in the Carajás mineral province, Pará State, Brazil

[1]Rosaline Cristina Figueiredo e Silva, [1]Lydia Maria Lobato, [1]Carlos Alberto Rosière, [2]Steffen Hagemann

[1]Universidade Federal de Minas Gerais, Centro de Pesquisas Prof. Manoel Teixeira da Costa-Instituto de Geociências. Av. Antônio Carlos 6627, Campus Pampulha, Belo Horizonte, MG, 31270.901, Brazil. Email: rosalinecris@yahoo.com.br,
[2]Centre for Exploration Targeting, School of Earth and Geographical Sciences, University of Western Australia, Australia, Crawley, Western Australia 6009

Recebido e 14 de novembro de 2011; aceito em 19 de novembro de 2011

ABSTRACT: The Carajás iron ore deposits, located in the southern part of the state of Pará in Brazil, are hosted by the metavolcano-sedimentary sequence of the Grão Pará Group, Itacaiúnas Supergroup. The protoliths to iron mineralization are jaspilites, under- and overlaid by basalts, both greenschist facies metamorphosed. The major Serra Norte N1, N4E, N4W, N5E and N5S iron ore deposits of the Carajás Mineral Province are distributed along, and structurally controlled by, the northern flank of the Carajás fold. High-grade iron mineralization (> 64 % Fe) is made up of hard and soft ores. The basal contact of the high-grade iron ore is defined by a hydrothermally altered basaltic rock mainly composed by chlorite and microplaty hematite. Varying degrees of hydrothermal alteration have affected jaspilites to form iron ores, from distal alteration zone, representing an early alteration stage, to intermediate and proximal alteration zones, synchronous with the main iron-ore forming event. The latter represents an advanced alteration stage (i.e., the high-grade iron ore). Jaspilites from the N4W, N5E and N5S deposits, and hard ores from N1 and N4E have a low ∑REE content, are enriched in light REE and exhibit positive europium anomalies (Eu/Eu*> 1), which is typical of Archean banded iron formations. The REE pattern defined by N5E ores is nearly flat and displays an increase in ∑REE and absence of the positive Eu anomaly. The increase in LREE was accentuated during the formation of magnetite and microplaty hematite, and the advance of martitization to form anhedral hematite, which may have favoured the relative increase of HREE in the residual fluid, resulting in an increase in HREE in advanced-stage precipitates and almost flat REE patterns associated with the advanced stage of mineralization (euhedral and tabular hematite formation). The mineralogical, geochemical and isotopic changes from jaspilites to high-grade iron ores suggests a hydrothermal origin for hard ore via interaction with an early-stage, relatively reduced magmatic fluid, which leached silica and formed magnetite, which evolved to more oxidizing conditions, with the advance of martitization, increase in the REE concentration and microplaty hematite precipitation in veins and martite borders , from interaction with modified meteoric waters.

Keywords: jaspilite, iron ore, Carajás, rare earth elements

RESUMO: ESTUDOS PETROGRÁFICOS E GEOQUÍMICOS DOS GIGANTES DEPÓSITOS DE MINÉRIO DE FERRO DA SERRA NORTE, PROVÍNCIA MINERAL DE CARAJÁS, PARÁ, BRASIL. Os depósitos de minério de ferro de Carajás, localizados no sudeste do estado do Pará no Brasil, estão hospedados na sequência metavulcanossedimentar do Grupo Grão Pará, Supergrupo Itacaiúnas. Os protólitos da mineralização de ferro são jaspilitos, soto- e sobrepostos por basaltos, ambos metamorfisados em fácies xisto verde. Os maiores depósitos de minério de ferro da Serra Norte são N1, N4E, N4W, N5E e N5S, estão distribuídos ao longo e estruturalmente controlados pelo flanco norte da dobra Carajás. Minério de alto teor (> 64 % Fe) consiste em minérios compactos e friáveis. O contato basal dos minérios de alto teor é definido por rocha basáltica alterada hidrotermalmente, composta por clorita e hematita microlamelar. Diferentes estágios de alteração hidrotermal afetaram jaspilitos para formar minérios de ferro, da zona de alteração distal, representada pelo estágio cedo-hidrotermal, às zonas de alteração intermediária e proximal, concomitantes com o evento principal de formação de minério de ferro. A zona proximal representa o estágio de alteração avançado (i.e., minério de ferro de alto). Jaspilitos dos depósitos N4W, N5E e N5S e minérios compactos dos depósitos N1 e N4E têm baixo conteúdo ∑ETR, são enriquecidos em REE leves e exibem anomalias positivas de európios (Eu/Eu*> 1), padrão típico de formações ferríferas bandadas arqueanas. O padrão de ETR definido por minérios de N5E é quase horizontal e apresenta aumento em ∑ETR e ausência de anomalia positiva de Eu. O aumento acentuado em ETRL ocorreu durante a formação de magnetita e hematita microlamelar. Já aumento em ETRP e padrão quase horizontal de ETR coincidem com o avanço da martitização formando hematita anédrica, o qual pode ter favorecido o aumento relativo de ETR pesados no fluido residual, resultando em precipitados do estágio avançado de mineralização (formação de hematitas euédrica e tabular). As mudanças mineralógicas, geoquímicas e isotópicas de jaspilitos a minérios de ferro de alto teor sugerem uma origem hidrotermal para minério compacto via interação de fluido magmático reduzido em estágio cedo-hidrotermal, lixiviando sílica e formando magnetita. Este fluido evoluiu para condições mais oxidantes, com avanço da martitização, aumento na concentração de ETR e formação de hematita microlamelar em veios e bordas de martita, a partir de mistura com águas meteóricas modificadas.

Palavras-chave: jaspilito, minério de ferro, Carajás, elementos terras raras

1. INTRODUCTION

The Carajás Mineral Province (CMP) is located in the eastern part of the Amazon craton, east-southeastern Pará State, Brazil (Fig.1), and is considered one of most important mineral provinces of the world, with production and growing potential for Fe, Mn, Cu, Au, Ni, U, Ag, Pd, Pt, Os, Zn and W. The iron ores are hosted by the Carajás Iron Formation, which is interbedded with mafic volcanic rocks of the Grão Pará Group of the Neoarchean Itacaiúnas Supergroup (Fig. 1). The Grão Pará Group outcrops along the northern and southern flanks of a synclinal structure, known as the Carajás fold, with a major shear zone known as the Carajás shear zone along the axis of the fold. Iron ore deposits developed along the northern flank of the fold, known as the Serra Norte (Northern Range) deposits and along the southern flank known as the Serra Sul (Southern Range) deposits (Fig. 1). At present, only

some of the Serra Norte deposits are mined with extensive exploration taking place in some of the Serra Sul deposits. There are nine deposits in the Serra Norte, numbered N1 – N9 (Figs. 1 and 2), with strike lengths from hundreds of meters to tens of kilometers and some of them comprise two or more orebodies. The combined resources of the nine deposits are 17.3 billion tons at 66 wt. percent Fe (CVRD, 2007), with orebody thicknesses varying from approximately 250 to 300 meters. Four main open pits (Figs. 2A and B) have, to date, produced about 1.2 billion tons of high-grade iron ore, which made Carajás the second largest Brazilian producer of iron following the Quadrilátero Ferrífero (Iron Quadrangle) region of Minas Gerais State (Rosière *et al.,* 2008).

Jaspilites constitute the protore in many iron ore deposits of the Carajás region (Meirelles, 1986). The term jaspilite was first applied in the Lake Superior area to name oxide-facies iron-formation in which silica is present as jasper (UNESCO, 1973). In Carajás, the term jaspilite was first used by Suszczynski (1972) to describe the banded iron formations (BIFs) in the Serra Norte deposits (Fig. 1). This type of BIF consists of bands of chert with hematite dust (*i.e.* jasper) intercalated with iron oxides. In this paper, and other contributions to the Carajás iron ore mineralization (*e.g.* Figueiredo e Silva, 2004; Figueiredo e Silva *et al.*, 2007a; b; 2008; Hagemann *et al.*, 2006; Lobato *et al.*, 2005a, b; 2008, Zucchetti, 2007; Zucchetti *et al.*, 2007), we use the term jaspilite as the BIF type described in the Serra Norte mines and surroundings. This BIF type is clearly different from BIF found in other parts of the Carajás area. A volcanogenic origin for these jaspilites is indicated by Meirelles (1986), Dardenne & Schobbehaus (2001, and references therein) and Klein & Ladeira (2002) based on the Grupo Grão Pará tectonic environment and/or the geochemical characteristics of the jaspilites. However, we stress here that we use jaspilite as a descriptive term with no genetic connotation.

The Carajás Range iron ore occurrences were discovered in August 1967 by Companhia Meridional de Mineração, the pilot area being the current N1 deposit (Beisegel *et al.,* 1973). In 1969, 18 mineral exploration license areas were claimed by Companhia Meridional de Mineração and Companhia Vale do Rio Doce (CVRD – now named Vale) encompassing some 160 000 ha area. From 1970 to 1972, an intensive exploration program was executed (Beisegel *et al.,* 1973). Open pit mining of the N4E deposit started in 1984, followed by the N4WC (central northwestern 4 orebody) in 1994, the N4WN (north northwestern 4 orebody) in 1996, and the N5W and N5E deposits in 1998 (Huhn *et al.,* 2000). Presently, all iron ore deposits belong entirely to Vale, the world's largest producer of iron ore (CVRD 2007). At the moment, the S11 orebody in the Serra Sul is the subject of an intensive exploration campaign.

Similar to other BIF iron ore districts in Brazil, such as the itabirites in the Iron Quadrangle in Minas Gerais State, jaspilites hosts soft (*i.e.* high porosity) and hard (*i.e.* low porosity) high-grade ores. Both supergene and hypogene genetic models explaining the formation of iron ores have been suggested (Morris, 1985). During the past 12 years, many research groups have studied iron ore deposits in Australia (Barley *et al.*, 1999; Hagemann *et al.*, 1999; Taylor *et al.*, 2001; Thorne *et al.*, 2004; Angerer & Hagemann, 2010), South Africa (Beukes *et al.,* 2002; Netshiozwi, 2002; Gutzmer *et al.*, 2006) and Brazil (Varajão *et al.*, 2002; Cabral *et al.*, 2003; Spier *et al.,* 2003; Rosière and Rios, 2004; Rosière *et al.,* 2008). Although these deposits contain hypogene iron mineralization, with silica leaching, with or without iron addition, most authors agree that supergene fluids are involved in the iron ore forming process as well. A few studies have proposed a hydrothermal origin for the Carajás hard iron ores, with hydrothermal introduction of *e.g.*, hematite, carbonate and sulfide (Guedes, 2000; Guedes *et al.,* 2002; Figueiredo e Silva, 2009; Figueiredo e Silva *et al.,* 2008; Dalstra and Guedes, 2004; Lobato *et al.*, 2005a, b). There is significant evidence, based on constraints of the paragenetic sequence and textural features, for the contemporaneous emplacement of veins and hydrothermal alteration in the jaspilite and also in the mafic wall rocks, which caused the transformation of jaspilites to high-grade ores, i.e., the mineralization process(es). This paper is only concerned with the formation of hard ores considered to be of hypogene origin and provides: (1) a reevaluation of the regional setting of the CMP, (2) descriptions of the main iron ore deposits, (3) the petrography and geochemistry of the protore and hard iron ores, (4) hydrothermal alteration zonation including vein classification and minerals that formed during the transformation of jaspilite to hard ores, and (6) an assessment of previous genetic models.

2. GEOLOGICAL SETTING OF THE CARAJÁS MINERAL PROVINCE

The Carajás Mineral Province (CMP) is divided into two Archean tectonic blocks, the southern Rio Maria granite-greenstone terraine (Huhn *et al.*, 1988) and the northern Itacaiúnas Shear Belt (Araújo *et al.*, 1988). The CMP is characterized by: (1) the giant iron ore deposits of the Serras Norte (N1 to N9), Sul (S1 to S45) and Leste , (2) the iron oxide-copper-gold (IOCG) deposits of Salobo, Pojuca, Alemão-Igarapé Bahia, Cristalino, Sossego, Alvo 118, and Gameleira; (3) the

gold-palladium deposit at Serra Pelada, (4) the manganese deposits at Azul and Sereno; and (5) the nickel deposit at Vermelho (Fig.1). The area covered by these deposits is characterized by metavolcano-sedimentary rocks, and Meso- to Neo-Archean basement, which consist of igneous suites and metamorphic complexes (Santos, 2003; Tassinari *et al.,* 2000).

In the northern Itacaiúnas Shear Belt, granite-gneissic terrains, such as the tonalite-trondhjemite-granodiorite (TTG) Xingu Complex (Silva *et al.,* 1974),form the basement underlying the volcano-sedimentary sequence. Many Archean granites intrude the basement and cover volcano-sedimentary sequences, such as the granites and diorites of the 2.74 Ga Plaquê Suite (Fig. 1) (Huhn *et al.*, 1999), and the foliated 2736 ± 24 Ma Planalto alkali granite (Avelar *et al.*, 1999; Huhn *et al.,* 1999). Mafic-ultramafic intrusive rocks are represented by the 2763 ± 6 Ma Luanga suite (Machado *et al.*, 1991).

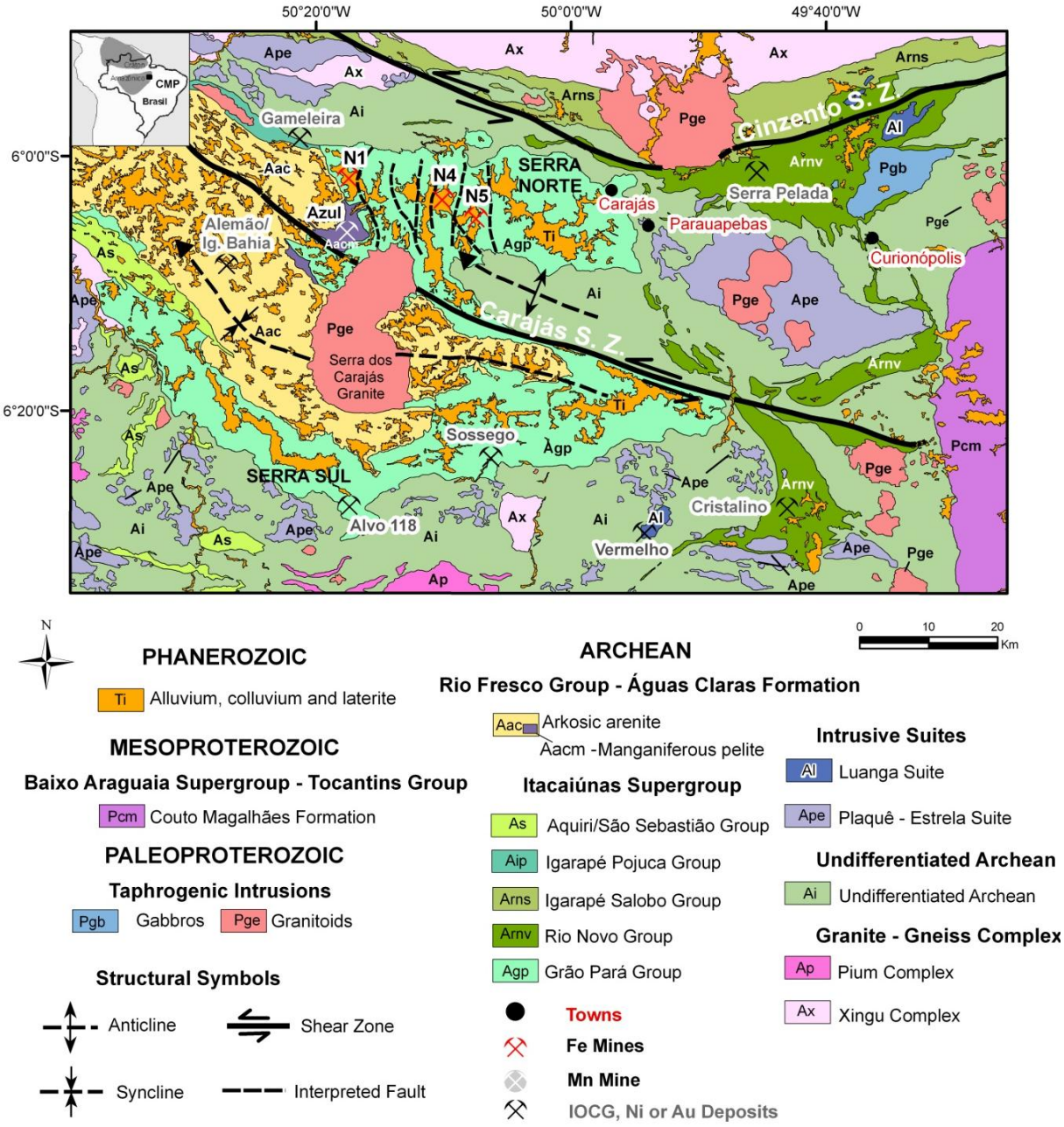

Fig. 1. Geological map of the Itacaiúnas Shear Belt, Carajás Mineral Province (after Bizzi et al., 2001) showing major mineral resources including iron ore deposits N1, N4 and N5 (Serra Norte), Serra Sul and Serra Leste; some IOCG deposits (Gameleira, Alemão/Igarapé Bahia, Alvo 118, Sossego, Cristalino); the Serra Pelada gold-palladium deposit; the Azul manganese deposit, and the Vermelho nickel deposit. Lithostratigraphic classification is adapted with field data from Costa (2007) and interpretation by Seoane et al., (2004), based on Landsat ETM7 RGB 321, 752 and PC1-52 images.

The Serra dos Carajás, the S-shaped mountain belt that contains the major iron ore deposits, itself is composed of metavolcano-sedimentary and metasedimentary rock units of the Itacaiúnas Supergroup (Fig. 1). In the northern part, the Itacaiúnas Supergroup includes greenschist facies metavolcano-sedimentary and metasedimentary sequences of the Igarapé Bahia (2745 ± 1 and 2747 ± 1 Ma; Galarza & Macambira, 2002), Aquiri, Grão Pará (Santos, 2003) and Rio Novo (*e.g.* Costa, 2007) Groups. In the south it includes the amphibolite-facies Igarapé Salobo and Igarapé Pojuca Groups (e.g., Lindenmayer, 1990). Despite their tectono-metamorphic overprint, these rocks commonly exhibit low-strain features, and original structures and textures may be preserved. Igneous or sedimentary terminology is widely used for these rocks and the prefix 'meta' is implicit but omitted for ease of reading in this manuscript.

The Grão Pará Group (Fig. 1) is a typical greenstone-belt succession composed of volcanic and sedimentary rocks with ages between 2.8 and 2.7 Ga (Gibbs *et al.*, 1986; Wirth *et al.*, 1986; Olszewsky, 1989; Macambira *et al.*, 1996; Trendall *et al.*, 1998) with interbeds of BIF. The lower unit of this Group, the Parauapebas Formation (Meireles *et al.,* 1984), consists mainly of basalts and basaltic andesites, and minor basic to intermediate pyroclastic rocks. An amygdaloidal facies is found closer to the top of the unit (Meireles *et al.,* 1984) with BIF and basic tuff intercalations. In the basal portions, rhyolite layers are found together with fluvial conglomerates and arenite. The rocks were subjected to regional greenschist metamorphism and hydrothermal alteration that caused iron enrichment (Figueiredo e Silva *et al.*, 2008; Zucchetti, 2007). The pyroclastic or volcanoclastic rocks preserve ocean-floor hydrothermal minerals, and this suggests very low-grade metamorphism (Zucchetti & Lobato, 2004; Zucchetti, 2007). Parauapebas Formation metabasalts that are devoid of hydrothermal alteration are composed of actinolite, chlorite, epidote, quartz, and calcite, also compatible with greenschist facies metamorphism (Meirelles, 1986; Macambira *et al.*, 1990; Teixeira & Eggler, 1994; Teixeira *et al.*, 1997).

The middle part of the Grão Pará Group is formed by the BIFs of the Carajás Formation (2751 ± 4 Ma; Krimsky *et al.*, 2002), which host the giant iron ore deposits (Tolbert *et al.*, 1971, 1973; Gibbs & Wirth, 1990). The Carajás Formation, defined in 1972 (DOCEGEO, 1988), contains layers and discontinuous lens-shaped bodies, or lenses, of jaspilites and high-grade iron ores, intruded by mafic sills and dikes. The mafic sills and dikes at the N4E deposit, varies from centimeters to tens of meters in width (Macambira & Silva, 1995). Jaspilites display typical intercalation of centimeter-thick, light and dark layers, or mesolayers (about 5 cm), and microlayers with iron-oxide layers intercalated with reddish to light-colored layers comprised of jasper and chert, respectively. Primary structures and textures in the jaspilites such as syn-sedimentary microfaults and spherulites (jasper or chert ringed by hematite) are still observed, despite the greenschist grade of metamorphism (Meirelles, 1986). Dolomite-bearing iron formations consist of layers of dolomite and chert in varying proportions, alternating with dark iron-oxide layers (Macambira & Schrank, 2002; Dalstra & Guedes, 2004). The dolomite-bearing iron formations are approximately 50 meters thick extending for about 400 m along strike.

In the central part of the Serra dos Carajás, the volcano-sedimentary rocks are covered by sedimentary psammo-pelitic rocks *(e. g.* arenites, calcarenites, siltites and conglomerates) of the Águas Claras Formation (Fig. 1), which yielded zircon U-Pb ages of 2708 ± 37 Ma (Mougeot, 1996) and 2645 ± 12 Ma (Dias *et al.*, 1996).

Paleoproterozoic A-type, alkaline to subalkaline granites such as the Serra dos Carajás granite (Fig. 1) intrude the Itacaiúnas Supergroup and have an age of about 1880 ± 2 Ma (Machado *et al.*, 1991). Dall'Agnoll & de Oliveira (2007) have classified these as oxidized, magnetite-series, rapakivi-type granites.

A Paleoproterozoic age for the iron mineralization has been constrained by whole-rock Sm-Nd data on hematitized mafic volcanic (basalt) wall rocks, along the contact with the high-grade iron ore (Lobato *et al.*, 2005b). More recently, Santos *et al.* (2010) obtained two distinct ages using hydrothermal minerals associated with the iron oxides of mineralized samples at N5E. Anatase in hematitized mafic volcanic rock yielded 1717 ± 12 Ma, and monazite included in hydrothermal hematite in iron ore indicated 1613 ± 21 Ma. These are interpreted as representing the iron mineralization ages.

3. TECTONIC AND STRUCTURAL SETTING

Several interpretations have been presented for the tectonic evolution of the Itacaiúnas Supergroup volcano-sedimentary sequence in the Carajás region. Dardenne *et al.* (1988) suggest a rift-related subduction zone to account for the basin responsible for the Grão Pará Group's evolution, which would have developed on continental crust adjacent to rift zones (Olszewsky *et al.*, 1989). Other authors point out that the volcano-sedimentary sequence is related to intracratonic basins (Gibbs *et al.*, 1986; Machado *et al.*, 1991; Lindenmayer and Fyfe, 1992; Santos, 2003; Grainger *et al.*, 2008), or that such

sequences formed in an arc environment of an evolving subduction zone (Meirelles & Dardenne, 1991; Teixeira, 1994; Lobato *et al.*, 2005b; Rosière *et al.*, 2006).

According to Zucchetti (2007) and Zucchetti *et al.* (2007), the Grão Pará Group basalts have a calc-alkaline magmatic affinity, and Nb-negative and Th-positive anomalies that are consistent with a subduction zone signature. Trace-element enrichment (*e.g.* high Zr/Y and Nb/Yb ratios) suggests that they formed in a continental-arc environment (Zucchetti, 2007). Basalts (Olszewsky *et al.*, 1989), and jaspilites with negative ε_{Nd} values (Lobato *et al.*, 2005b) indicate crustal contamination of the Grão Pará sequence. Thus, the trace-element geochemistry characteristics suggest a back-arc-related tectonic setting on an attenuated continental crust (Zucchetti, 2007; Zucchetti *et al.*, 2007). These authors also suggested that the Grão Para Group is a greenstone-belt-type sequence as previously indicated by Hirata *et al.* (1982), Meireles *et al.* (1984), Araújo & Maia (1991) and Faraco *et al.* (1996).

The structural setting of the CMP is extensively discussed in the literature (Beisegel *et al.*, 1973; Silva *et al.*, 1974; Araújo and Maia, 1991; Holdsworth & Pinheiro, 2000; Pinheiro & Holdsworth, 1997; 2000) despite a distinct lack of detailed field data. A summary of the structural framework was provided by Rosière *et al.* (2006) who proposed that the dominant structure is a flattened flexural fold system with axes moderately plunging ESE to WNW, intersected by several strike-slip faults that trend sub-parallel to the fold plane of the fold system. This interpretation is based on structural data taken from several iron ore deposits (N1 to N5), regional mapping and satellite image analyses. Further to the southeast (N6 to N8), other Serra Norte deposits are currently being investigated in order to better define the regional structural setting including the anticlines and synclines.

The Serra dos Carajás itself is a S-shaped syncline-anticline pair, named the Carajás fold, and is partially disrupted by the Carajás shear zone. The latter divides the entire structure into blocks that subsequently were named the Serra Norte and Serra Sul (Fig. 1). The approximately WNW-ESE-trending sinistral Carajás and Cinzento shear zones (Fig. 1) represent major structural discontinuities sub-parallel to the axial plane of several minor regional folds. The shear zones were likely developed to accommodate progressive flattening of the Carajás fold by lateral escape (Rosière *et al.*, 2006). Another major event that influenced the structural setting of the area, particularly in the eastern part of the CMP, was the intrusion of shallow-level (Barros *et al.*, 2001), syntectonic calc-alkaline granite intrusions (named intrusive suites in Fig. 1), such as the Estrela Complex (Barros & Barbey, 1998, 2000), into the metamorphosed volcano-sedimentary sequences of the Itacaiúnas Supergroup.

The Carajás and Cinzento shear zones (Fig. 1) played a decisive role in the iron mineralization processes by preparing the terrane (*i.e.* increased the porosity) during the Archean and creating pathways for hydrothermal fluids to percolate in the Proterozoic when these shear zones were reactivated, resulting in roughly north-south splays along the Serra Norte iron ore deposits.

The high-grade Serra Norte orebodies developed in zones of greatly enhanced rock permeability at the regional hinge zone of the anticlinal Carajás fold (Rosière *et al.*, 2006), which has been subsequently disrupted and rotated by faults and related splays. Hard orebodies surrounded by soft ore are preferentially concentrated in the hinge zone of large folds such as in the N5 deposit (Lobato *et al.*, 2005a). The Serra Sul deposits are located within large (i.e., hundreds of meters to kilometer wavelength) second-order folds (Lobato *et al*, 2005b), but the detailed structural framework and relative timing relationships are presently not well constrained.

According to Rosière *et al.* (2006) and Lobato *et al.* (2005b), the formation of the Carajás iron orebodies postdated regional metamorphism and all Archean deformation events documented in the CMP. Regional metamorphic grade is very low in rocks of the Grão Pará Group (*e.g.* Beisiegel *et al.*, 1973; Gibbs *et al.*, 1986). Medium- to high-temperature minerals and tectonic fabrics in both ore and country rocks are found exclusively in: (i) the shear-zone domains, where high hydrothermal fluid-to-rock ratios control the mineral assemblages, or (ii) the contact metamorphic zones near granitic bodies. Most of the granites in the CMP and near the iron ore deposits are of Proterozoic age (*e.g.* Machado *et al.*, 1991). High-grade iron ores also display a distinct hydrothermal texture, such as comb-textured hematite veins and breccias, which overprints the jaspilite fabric.

4. IRON ORE DEPOSITS

4.1 - Mesoscopic classification of iron ore types

The protore at the Serra Norte iron ore deposits is defined as: (1) jaspilite, which may contain bedding-parallel quartz veins, and (2) early-stage hydrothermally altered, so-called, least-altered jaspilite. Iron ore is defined as advanced stage hydrothermally altered and mineralized jaspilite and consists of hard- and porous hard-ore. Hard ore also includes variable amounts of quartz +/– hematite vein types. Soft ores can be the direct product of

jaspilite and hypogene ores via supergene enrichment (Tolbert, 1971), but these are not described here. The transition from the jaspilite to the hydrothermal hard ore encompasses the development of varying porosity stages that may locally characterize a high-grade soft ore type (Lobato *et al.*, 2005a; 2008). This type of hypogene soft ore is typical of the N4E deposit.

High-grade ores can be both soft and hard, and are classified in terms of their physical hardness into hard to medium-hard, friable, soft and powdery and dusty ore (Clout & Simonson, 2005). Hard to medium-hard ores have a low porosity with an interlocking texture between martite and hematite, or martite-MpHem (microplaty hematite) grains. Friable ores are easily disintegrated by hand, and are more porous than medium-hard ore. They commonly break into centimeter-size prisms/plates, defined by joint planes and fissile beds. Soft (0.05-1.0 mm particles) ores are those that can be dug in situ by hand or with a shovel; they are very porous, but typically not powdery. Soft orebodies are discontinuous and tabular, friable and banded, and locally contain massive hard ore lenses.

The friable ore displays primary lamination and contains 64 to 67 wt per cent Fe. It consists of friable hematitic material with gray color, metallic luster and a high porosity. High-grade hard ores may be massive, and/or compact, brecciated and banded where the layers can be compact and/or porous (Rosière & Chemale Jr., 2000). Locally, the brecciated ores exhibit fragments of dissilicified jaspilite layers, with the original fabric completely destroyed in places (Figueiredo e Silva, 2004). Compact hard ores, commonly gray blue, contain 67 wt percent Fe, have a metallic luster and low porosity. Massive hard ores are mainly observed along the contact between jaspilites and lower basaltic wall rocks as small lenses and tabular bodies (first described by Tolbert *et al.,* 1971), and also as lenses surrounded by basaltic rock.

Basalts in the N4 and N5 deposits display hydrothermal alteration minerals, with both intense chloritization and hematitization along the contact with the orebody (Figueiredo e Silva, 2004; Zucchetti, 2007).

Iron ores and weathered basaltic rocks are covered by ferricrete (*canga*), which formed in the superficial portions of deposits as a supergene product. It consists of cemented goethitic/limonitic material, with colloform, vuggy textures, and has a high porosity. Where *canga* is located directly over iron ore, it consists of hematite blocks that are cemented by hydrated iron oxides (Lopes, 1997). The classification and description of the supergene ores are provided in Beisegel *et al.* (1973), Rezende & Barbosa (1972) and Ladeira & Cordeiro (1988).

Iron ore may be contaminated with: (i) manganese, particularly where in contact with lower basaltic wall rocks; (ii) aluminum and phosphorous where in contact with *canga*; and (iii) silica, which generally increases with depth (CVRD, 1996). The cut-off grade for iron ore is 60 wt % Fe, 2 wt % Mn, 2-2.5 wt % Si and Al, and 0.2 wt % P.

4.2 - Geological setting of the N1, N4 and N5 deposits

N1 deposit: At the N1 deposit (Fig. 2A), the dip of the rocks of the Carajás Formation varies from 45° to subvertical and outcrops are characterized by soft friable ore, soft lateritic hematite ore and *canga* cover. Hard ore is subordinate to soft ore and is found as either discordant (northeastern part of the N1 deposit) vein-controlled or concordant (southeastern part of the deposit) lenses to the soft ore. Hard ore may contain hematite veinlets.

N4 deposit: The N4 deposit comprises two main orebodies, namely N4E and N4W that are interpreted to be separated by a N-S oriented fault (Fig. 2B). The N4W orebody (Fig. 2B) is presently the most important in the Carajás iron district, with total reserves in excess of 0.5 billion tons, and consists mainly of soft ore and only minor hard ore. Bodies of hard ore are frequently close to NE-SW and NW-SE trending faults (Domingos, 2005). Jaspilites (Fig. 5A) have an average thickness of 220 meters (Borges, 1994) and crop out in the northern portion of the N4E deposit as well as smaller, < 40 meters thick lenses contained within the orebodies. Phosphorus, aluminum and manganese contents increase close to ferricrete cover, and along contacts with mafic volcanic wall rock and dikes (CVRD, 2004).

The N4E open pit displays an approximate J shape structure in plan-view (Fig. 2B), with a N-S extension of 5 km, width of about 500 m and an average orebody thickness of 350 m. The deposit is divided into a northern and southern domain. In the northern domain the lithological units strike mainly N-S and dip to the W. According to Ladeira & Cordeiro (1988), hard hematite orebodies and jaspilites are distributed discontinuously along a N30W trend in the northern domain of the N4E deposit, which is also the trend of the axial trace of early-stage folds (F1). The second-generation F2 folds plunge 4° toward N25-50W. Laminated soft ore predominates in the northern domain, containing many irregular and partially preserved jaspilite lenses. Lenses of hard ore are in the middle of soft ore (Fig. 4A) that is in contact with jaspilite. The jaspilites contain concordant and discordant quartz veins, as well as hematite veinlets with quartz nuclei. The soft ore contains hematite veinlets and is locally brecciated at the basal contact with basaltic rocks.

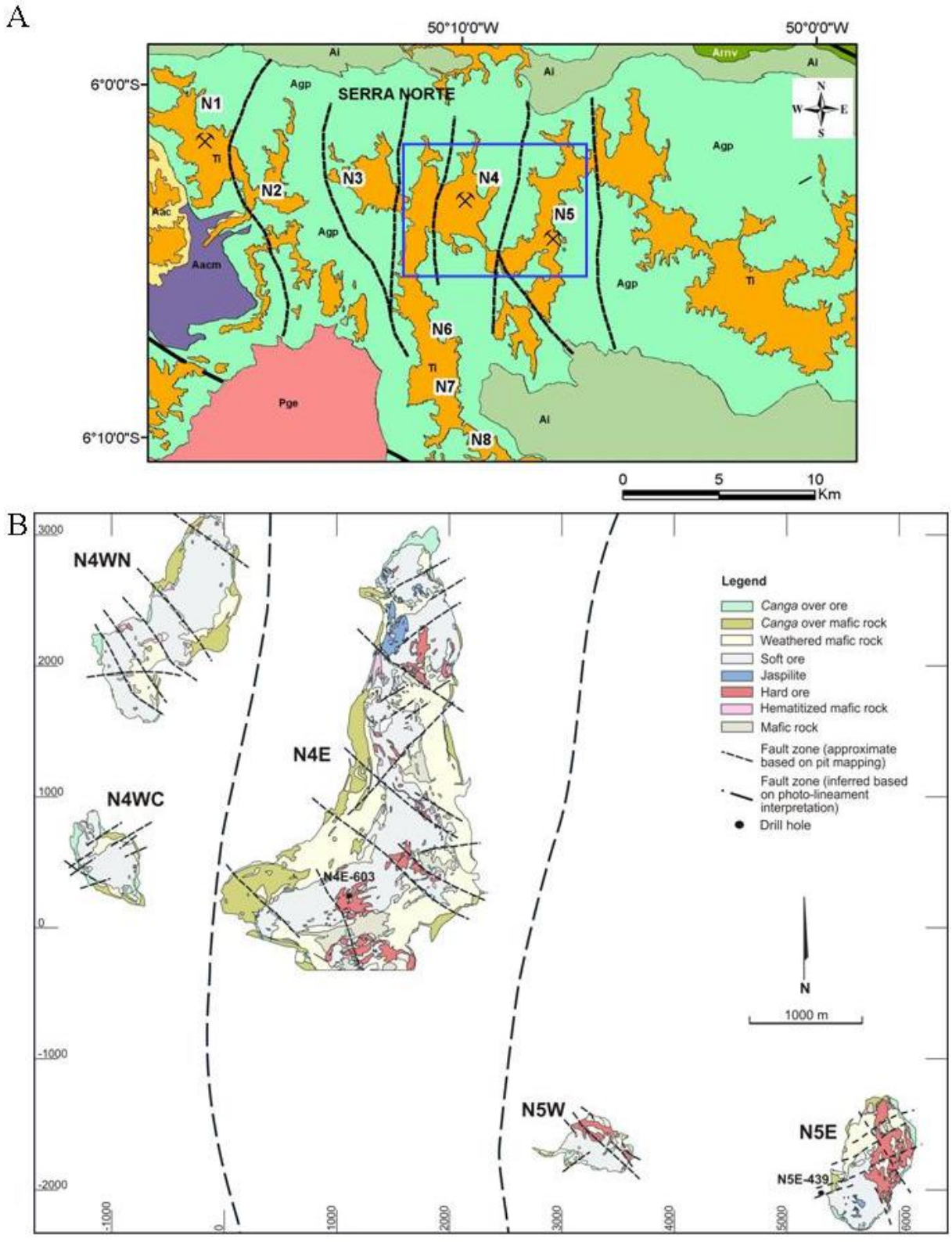

Fig. 2. A. Location of Serra Norte N1 to N8 deposits. Blue square represents area detailed in B (Refer to figure 1 for legend). B. Schematic geological map obtained from drill core and open pit mapping of the N4WN, N4WC, N4E, N5W and N5E deposits.

At the N4W deposit, soft ore predominates and hard ore is scarce. The soft ore consists mainly of friable and porous hematite-martite material. The open pit is approximately 7 km long, 200 to 500 m wide and 400 m deep (CVRD, 1996). The bedding of jaspilites and ores strike NW-SE with variable dips from subvertical to 40°-50° to the SW in the central part of the open pit. In the northern part of the open pit bedding strikes N20-30E, and dips 40°-50° to the NW (Pinheiro *et al.*, 2001). Poles of these structures indicate major mine-scale folds with their axes plunging shallowly (< 30°) to the NW (Pinheiro *et al.*, 2001). A gradational soft ore and jaspilite contact is often observed in many of these mine benches (Fig.

5D). Quartz breccias (hematite-free), as well as bedding-discordant quartz veins, are commonly observed.

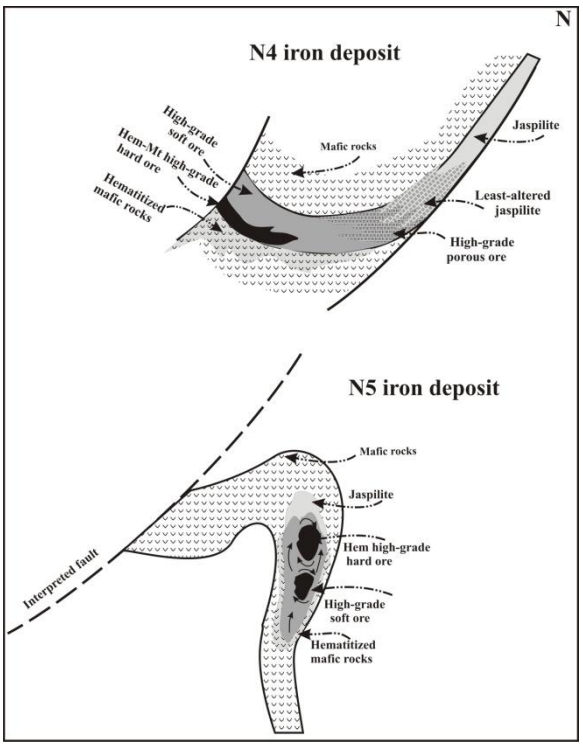

Fig. 3. Schematic illustration of the geological setting of the N4 and N5 deposits (Modified after Lobato et al. 2005a). The upper diagram represents the Serra Norte N4 deposit, which contains a large amount of the porous, high-grade soft hematite-type ore with lenses of hard ore. They are in contact with least-altered jaspilites and mineralized mafic rocks. The lower scheme depicts the N5 ore deposit, where the high-grade hard hematite-type ore is abundant. Mineral abbreviations: Hem: hematite; Mt: martite; Mag magnetite.In the southern domain bedding planes strike NE-SW and dip to the NW, giving the J shape of this deposit (Pinheiro et al., 2001). Soft ore also predominates in the southern domain, enclosing lenses of dolomite-bearing and manganiferous jaspilites and, banded hard ore that contains dolomitic carbonate veins (Fig. 5B). Hydrothermally altered, hematitized basaltic rocks are found in the eastern portion of this domain at the lower contact of jaspilite with the ore sequence. Near the contact with the iron ore, the basalts are totally replaced by chlorite and hematite (up to ~ 80 vol % of chlorite and 15-20 vol % of hematite) and minor quartz, calcite, and white mica. Hard hematite orebodies (>66 wt % Fe) occur mainly near the contact with the underlying mafic metavolcanic rocks. They are typically surrounded by a hydrothermal aureole, which may contain hydraulic breccias; vugs filled with carbonate, quartz, kaolinite, MpHem, quartz-hematite veins (Fig. 5C), and fibrous chlorite aggregates (Guedes 2000). Carbonate-sulfide veins are known to be present along the jaspilite-basaltic lower contact (Figueiredo e Silva et al., 2007b) in the southeastern portion of the N4E deposit.

N5 deposit: The N5 deposit (Figs. 2 and 3) displays geological characteristics, such as the dominance of massive hard ore overlying soft ore that are distinct from those at the N4 deposit. The N5E orebody is presently pod shaped, with jaspilites and high-grade ore, mainly hematite, surrounded by mafic rocks, which are locally hematitized where in contact with hard ore (Figs. 3 and 4B). The jaspilites and basaltic rocks have a predominantly N40W to N80W strike and dip 50^{o}-60^{o} to the SW (Pinheiro *et al.*, 2001). Numerous, metallic gray hematite, stockwork veins may constitute hard ore and locally crosscut both the soft ores and jaspilites (Fig. 5E). "Christmas-tree" veinlets are also observed (Guedes *et al.*, 2002), similar to those described by Taylor *et al.* (2001) and Thorne *et al.* (2004). Evidence of dolomitic ore has only been noted in drillcore where dolomite veinlets crosscut and/or are parallel to beds, and locally forms a carbonate-rich breccia fill (Figueiredo e Silva, 2004; Figueiredo e Silva *et al.*, 2007a). The contacts between basaltic rock and hard ore, and jaspilite and porous hard ore, are gradational with clear lateral bedding continuity. The soft ore is enriched in silica near jaspilite lenses. Phosphorous contamination increases toward the ferricrete cover, whereas aluminum and silica increase towards the base of the orebody (CVRD, 2004). Discordant quartz veins are rarely associated with the hard ore. Zucchetti (2007) reported basaltic rocks that are completely replaced by chlorite and hematite where in contact with the iron orebodies (Figs. 5F and G). Late-stage hematite veins crosscut the chlorite-hematite rocks (Fig. 5H). At the N5S deposit, jaspilites are crosscut by vuggy quartz-hematite, and hematite-only veins that are either discordant or parallel to the jaspilite beds (Fig. 5I). Soft ore predominates and silica contamination is common. The most common hard ore in the N5S deposit constitutes meter-scale banded, silica-contaminated ore. This ore differs from the typical hard ores (which are scarce in N5S) in other deposits because it contains remnants of strongly desilicified and hematitized jaspilite-like bands. Hard magnetite-rich lenses (approximately 2m thick) are unique in the Serra Norte iron ore deposits, and are found locally at the jaspilite-ore contacts. Magnetite is also found as veins that are discordant or parallel to jaspilite beds (Fig. 5J).

5. PETROGRAPHY OF JASPILITE AND HARD IRON ORE

5.1 - Jaspilite and least-altered jaspilite

Jaspilite is characterized by alternating micro- to mesolayers (2 to 40 mm) of jasper and microcrystalline hematite (MiHem). The jasper layers (Fig. 6A) contain chert and dusty hematite, which is defined as <0.004 mm hematite particles. Locally the jasper layers contain chalcedony spherulites (0.01 to 0.1 mm in diameter). The MiHem layers (Fig. 6B) are composed of dense concentrations of very fine-grained, <0.004 mm,

hematite crystals that represent the original oxide species of the jaspilite bands.

Least-altered jaspilite contains portions of hematite-free, recrystallized chert in equilibrium with magnetite, interpreted as the early stage of hydrothermal alteration. Variably altered jaspilites may be brecciated, containing various amounts of hematite types (*e.g.* microplaty and anhedral), and vein-associated quartz, carbonate and sulfide minerals.

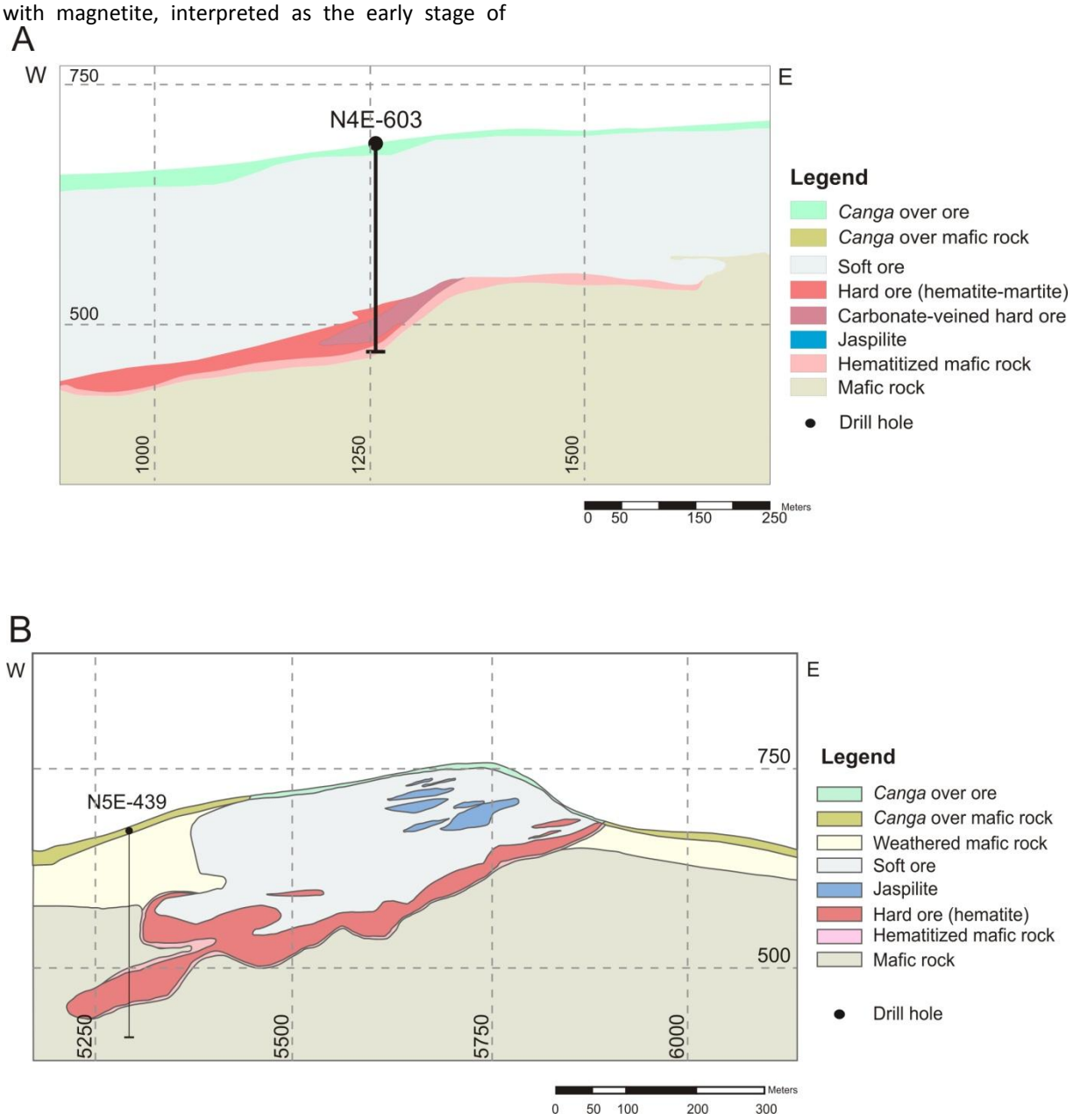

Fig. 4. A. Cross-section of the N4E orebody. B. Cross-section of the N5E orebody. Note the presence of a lens of hard ore along the contact with iron-mineralized mafic rock. Source Vale (local mine grid). For location of drill cores refer to figure 2B.

5.2 - Iron Ores

Iron ores are classified based on the oxide paragenetic sequence and detailed texture and mineralogy of oxides and gangue minerals such as quartz and carbonate (Table 1 and Fig. 7). Two main ore types are recognized: (i) hematite-martite (Figs. 7A, B and C), and (ii) hematite ores (Figs. 7D and E). Locally, the major ore types may develop certain variations, as shown in Table 1. Ores from the N4E deposit, for example, are characterized by a combination of different hematite types and martite, and may preserve layering (Fig. 7A) inherited from the jaspilitic protore; such ores may exhibit a continuous transition from a typical hard to a porous hard ore. The martite-hematite hard ore with quartz veins (Figs. 7C and H) has only minor amounts of carbonate. In contrast, carbonate and hematite-martite ores (Figs. 7B and G) contain

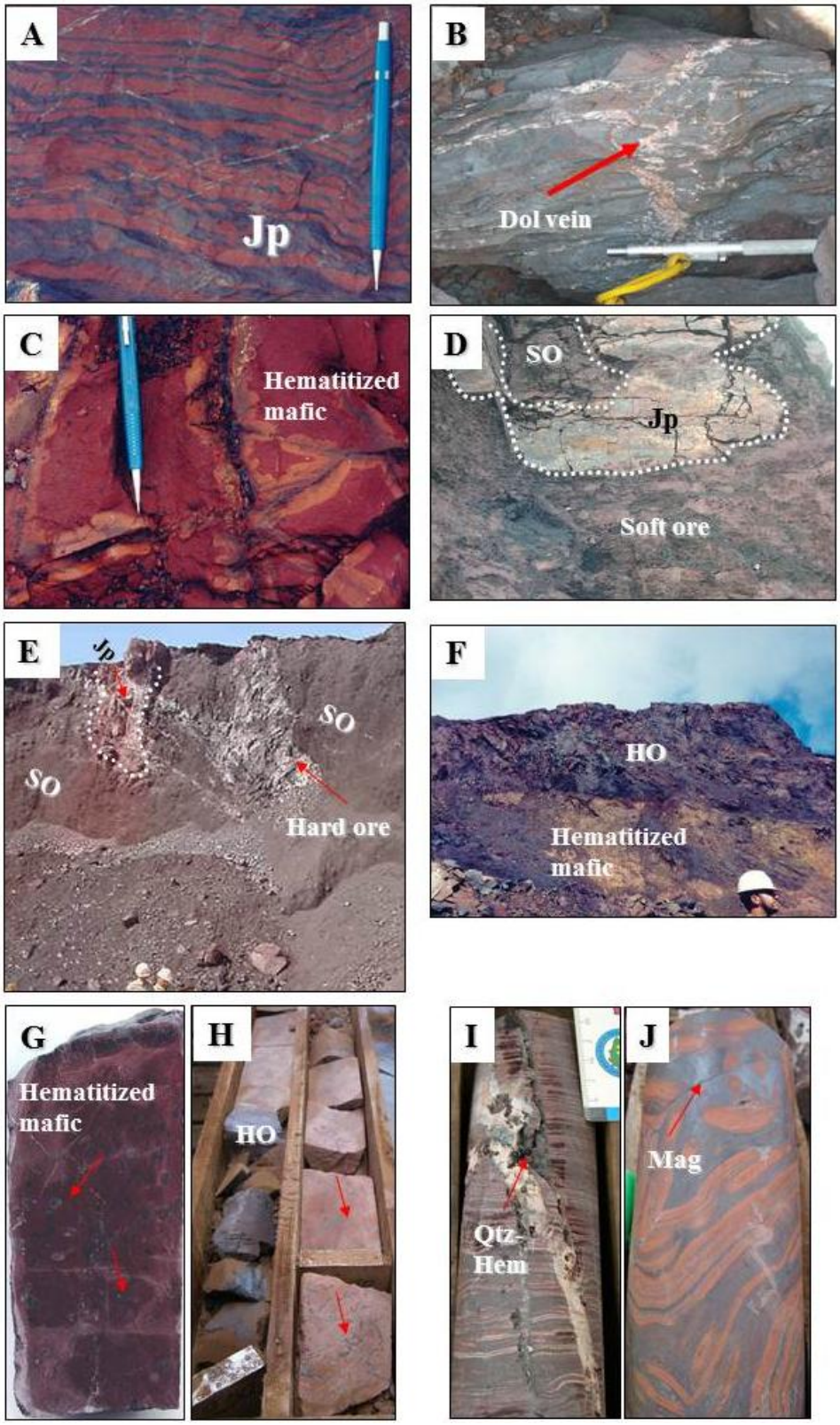

Fig. 5. A. Jaspilite (Jp) in the N4E northern domain. Microbanding is defined by alternating jasper and iron oxides bands. B. High-grade massive ore with carbonate veins discordant (arrow) and along bedding in the N4E southern domain. C. Mafic rock partially hematitized with hematite veinlets, N4E deposit. D. Gradational contact between jaspilite and soft high-grade ore (SO) in N4W deposit. E. Hematite hard ore stock-work veins crosscutting soft ore and also jaspilite lens, N5E deposit. F. Hematitized basaltic rock in contact with hard orebody, N5E deposit. G. Core sample of hematitized basaltic rock where amygdales are replaced by hematite (arrows), N5E deposit. H. Core samples showing contact between hard ore and basalt replaced by chlorite and hematite, with hematite veinlets (arrow), N5E deposit. I. Core sample of banded jaspilite from the N5S deposit showing quartz-hematite vuggy veins (arrow) cutting across the bedding in the jaspilite. J. Core sample of jaspilite from N5S deposit showing magnetite veins (arrow) cross-cutting the jaspilite. Abbreviations: Jp = jaspilite; SO = soft ore; HO = hard ore; Dol = dolomite; Qtz = quartz; Hem = hematite; Mag = magnetite.

significant amounts (up to 70 vol %) of carbonate (Figs. 7B and G). The ores of the N5E deposit differ from those of other deposits because they are brecciated and comprised almost entirely of hematite, i. e., massive or porous hard ore (Figs. 7D and J), representing those hard ores where the original layers were almost obliterated (Figs. 7 I, J and K).

Hematite-martite ore type: This ore type is typical of the N4E and N1 deposits. Hematite-martite ore is mainly composed of microcrystalline (+/– microplaty) hematite and disperse euhedral martite crystals with or without MpHem. Most of these ores still preserve the original jaspilite texture. Euhedral martite crystals are about 100 to 300 μm in size (Fig. 6D) and overgrow the massive MiHem and/or MpHem. Locally, kenomagnetite relics are present. Microplaty (or lamellar) hematite is made up of platy crystals, commonly with diamond-shaped sections of approximately 4-8 μm, locally up to 100 to 200 μm in length. The MpHem generally occupies vein walls (Fig. 6E), grows at the expense of martite (Fig. 7F), and less commonly is found in the center of martite crystals. Anhedral hematite (AnHem) forms eye-shaped agglomerates of lobate crystals in the oxide layers and also in veins. The crystals are ~ 20 μm in size and where located in veins, they display growth lamellae (Fig. 6F). Euhedral and bladed-tabular (EHem-THem) hematite occurs in veins, is fine- to medium-grained (200 to 300 μm) and forms internal selvages to veins (Fig. 6G). Microcrystalline hematite is recrystallized, where in contact with these EHem-THem hematite veins.

Hematite ore type: These ores are typical of the N5E deposit and are essentially composed of hematite, mainly microcrystalline (<0.004 mm), besides AHem, MpHem, EHem (+/– 0.3 mm) and THem (0.2-0.3 mm) (refer to Table 1 for explanation of abbreviations). These ores are generally brecciated, but locally preserve the original micro- to meso-bands that, if present, are defined by the intercalation of continuous and/or discontinuous layers of fine-grained (+/–0.03 mm) AHem aggregates with MiHem. The latter hematite can be recrystallized at the contact with MpHem-THem veins. Anhedral hematite mesobands are locally discontinuous and interspersed with vugs that may contain MpHem. The EHem-THem is commonly comb textured, may exhibit growth lines, and partially fill open spaces or vugs.

Hematitized wallrock: It consists of hydrothermally altered and mineralized basalt, which are found only at the contact between the mineralized jaspilite and the under- and overlying basaltic wallrock. In the N4E deposit, they are composed of talc, kutnahorite, quartz and rare chlorite (locally in veinlets) together with MpHem (up to 0.4 mm) (Fig. 6H), with subordinate anhedral crystals of martite. The EHem-THem veinlets crosscut these rocks and exhibit growth lamellae. At the N5E deposit, the hydrothermally altered basalts are composed of chorite (60%), with rare white mica, and MpHem (+/–35%) and martite (+/–5%). Rare kenomagnetite relics are present and locally also platy hematite with crystals up to 0.2 mm in length.

6. HYDROTHERMAL ALTERATION

Varying degrees of hydrothermal alteration have affected jaspilites, causing the transformation to iron ore, defined by a distinct paragenetic sequence of iron-oxide minerals with concomitant removal of silica and formation of a specific suite of veins that may contain quartz, carbonate, hematite, sulfide, monazite, and rare gold. The distal alteration zone represents an early alteration stage, whereas the intermediate and proximal alteration stages are synchronous with the main iron ore forming event. The proximal alteration stage also represents the advanced alteration stage, *i.e*., the high-grade ore itself. The distal alteration zone (up to ~ 80 m wide in the N4E deposit and ~ 100 m in the N4W deposit, measured vertically) in jaspilite is mainly characterized by the recrystallization of jasper and the removal of its iron, and the associated formation of magnetite (Fig. 8A). Magnetite crystals are euhedral to anhedral and form: (i) overgrowths on MiHem layers (Fig. 6C), (ii) grains in the nuclei of recrystallized chert invariably associated with crosscutting quartz veins, or (iii) grains in equilibrium with vein quartz and calcite. Magnetite is commonly replaced by hematite (martitization), leaving kenomagnetite relics (confirmed by Mössbauer analyses according to Figueiredo e Silva, 2004), which is a deficient Fe^{+2} magnetite phase (Kullerud *et al.*, 1969). Sulfides such as pyrite, chalcopyrite (Figs. 8C and D) may be associated with the hydrothermal alteration, but it should be noted that relatively rare, syngenetic pyrite (N4W) and calcite (N4E) crystals also occur in parallel laminae of jaspilite (Fig. 8B). The veins formed in this alteration zone lack hematite. The intermediate alteration zone is about 200 m in width (*e.g.* in the N5S deposit) and is characterized by martite, with or without kenomagnetite. Quartz-hematite and hematite-quartz veins are common (Fig. 8E) and contain MpHem and subordinate sulfides. The porosity increase in the altered jaspilites is significant, and affects the original jasper layers. The proximal alteration zone, represented by hard and hard porous ores, is about 20 to 50m in width. The original shape of martitic magnetite “blasts” is destroyed by the progressive martitization, forming AHem (Table 1) in abundant eye-shaped agglomerates of lobate crystals. Intense carbonate

alteration associated with the high-grade ores results in the formation of ore breccias cemented by dolomite. Examples are locally observed in the N5 deposit, and as kutnahorite cemented breccias in the N4 deposit. Hard ore with predominance of late-stage anhedral and tabular hematite lack quartz and carbonate veins. The presence of carbonate is mostly restricted to ores at depths >200 meters in the N5E deposit, and along the jaspilite-basaltic contact in the N4E deposit.

Microcrystaline hematite is stable even in the more advanced hydrothermal alteration stages. Stockwork-type veins contain tabular hematite. These zones are also characterized by discontinuous quartz ± carbonate veins with intergrown MpHem, which may be included in the hematite-martite ore type. The MpHem intergrown with quartz forms the matrix of hydrothermal breccias in the proximal alteration zone (Fig. 9F).

Hydrothermal alteration of basaltic wallrock has also been subdivided into intermediate and proximal alteration zones (Zucchetti, 2007). The hydrothermal zones are characterized by chlorite and chlorite-hematite replacement of the igneous minerals, respectively. The intermediate alteration zone has abundant chlorite, calcite, quartz, hematite, white mica, albite, titanite, magnetite, and subordinate sulfide minerals. Chlorite and MpHem from the proximal alteration zone occur along veins, or replace amygdales (Figs. 8G and H). Quartz, white mica, albite, titanite, and calcite are subordinate. The intermediate zone can locally extend up to about 30m, whereas the proximal zone is approximately 60m wide relative to non-altered basaltic rock (Fig. 5C).

Table 1. Hard iron ore types characteristics.

		Ore types				
Main types		**Hematite-martite**			**Hematite**	
		Hematite-martite (Hard Ore - HO**)**	Martite-hematite (brecciated HO)	Carbonate and hematite-martite (banded and brecciated HO)	Veined hematite (banded and/or brecciated HO)	Hematite and carbonate (brecciated HO)
Deposits		N1 and N4E	N4E	N4E	N5E	N5E
Mineralogy	**oxides**	MiHem, Mt (KenoMag), MpHem (±THem)	Mt (KenoMag), MiHem, MpHem, AHem-THem	Mt, MpHem, MiHem	MiHem, Sub-AHem, EHem-THem MpHem	AHem-EHem-THem, MpHem (filling porous), MiHem.
	sulfides	absent	absent	absent	Ccp	absent
Veins-Veinlets		(i)Qtz-Chalc, (ii)Qtz-Kut, (MpHem), (iii) MpHem + AHem, aside from AHem + THem*, (iv)Qtz-Talc-PlatyHem, (v)LamellarHem	Qtz-Kut-MpHem	Kut-Qtz; Carb-Qtz-MpHem	Qtz; MpHem-THem*; AHem-EHem	Dol
Others		Some samples are essentially composed by MpHem and Mt (Kmag), where MpHem is (i) fine-grained (< 5 µm) and (ii) coaser-grained (140 µm)	Pyramidal Qtz (up to 4 mm); AHem-THem overprint massive aspect.	Kut (cal) can constitute up to 70 %; Kut zoning is defined by fine hematite dust in triangular and rhombohedral forms.	Rare Au particle included in hematite; Coarser-grained (300 µm) AHem with growth lamellae.	Original banding is the most obliterated, together with veined-hematite association.

**In MiHem-rich bands, MiHem is coarser-grained and recrystallized at the contact with these veinlets. Mineral abbreviations: MiHem = microcrystalline hematite; Mag = magnetite; KenoMag = kenomagnetite; MpHem = microplaty hematite; Mt = martite; AHem = anhedral hematite; EHem=euhedral hematite; THem = tabular hematite; Ccp = chalcopyrite; Qtz=quartz; Kut=kutnahorite; Cal=calcite; Dol=dolomite*

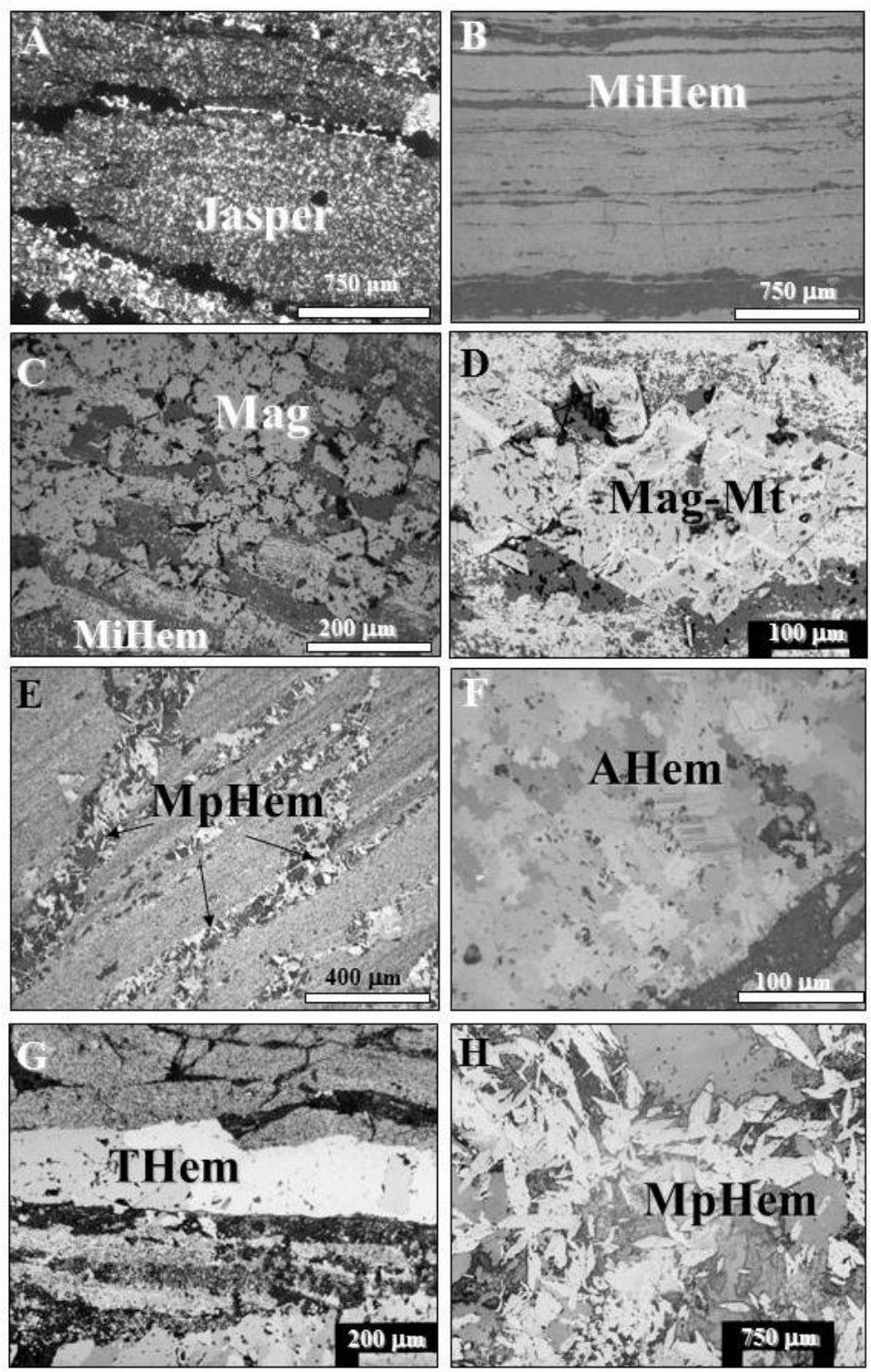

Fig. 6. Photomicrographs of jaspilite and ore. A. Jasper bands, rich in microcrystalline (or dusty) hematite, and recrystallized quartz in altered jaspilite, N4W deposit. Transmitted light, under crossed polars (25X). B. Bands of microcrystalline hematite in jaspilite, N4E. Reflected light (25X). C. Bands of microcrystalline hematite that is overgrown by magnetite, N4E deposit. Reflected light (100X).D. Magnetite partially oxidized to martite, N4W deposit. Reflected light (200X).E. Microplaty hematite developed along cavity/veinlets in brecciated hard ore, N5E deposit. Reflected light (50X). F. Anhedral hematite crystals with lobate borders in high-grade hematite ore, N5E deposit. Reflected light, under crossed polars (200X). G. Tabular hematite vein in brecciated N5E hematite ore. Reflected light, under crossed polars (100X). H. Microplaty hematite crystals in mineralized mafic rock. Reflected light, under crossed polars (25X). Mineral abbreviations: MiHem = microcrystalline hematite; Mag = magnetite; MpHem = microplaty hematite; Mt = martite; AHem = anhedral hematite; THem = tabular hematite.

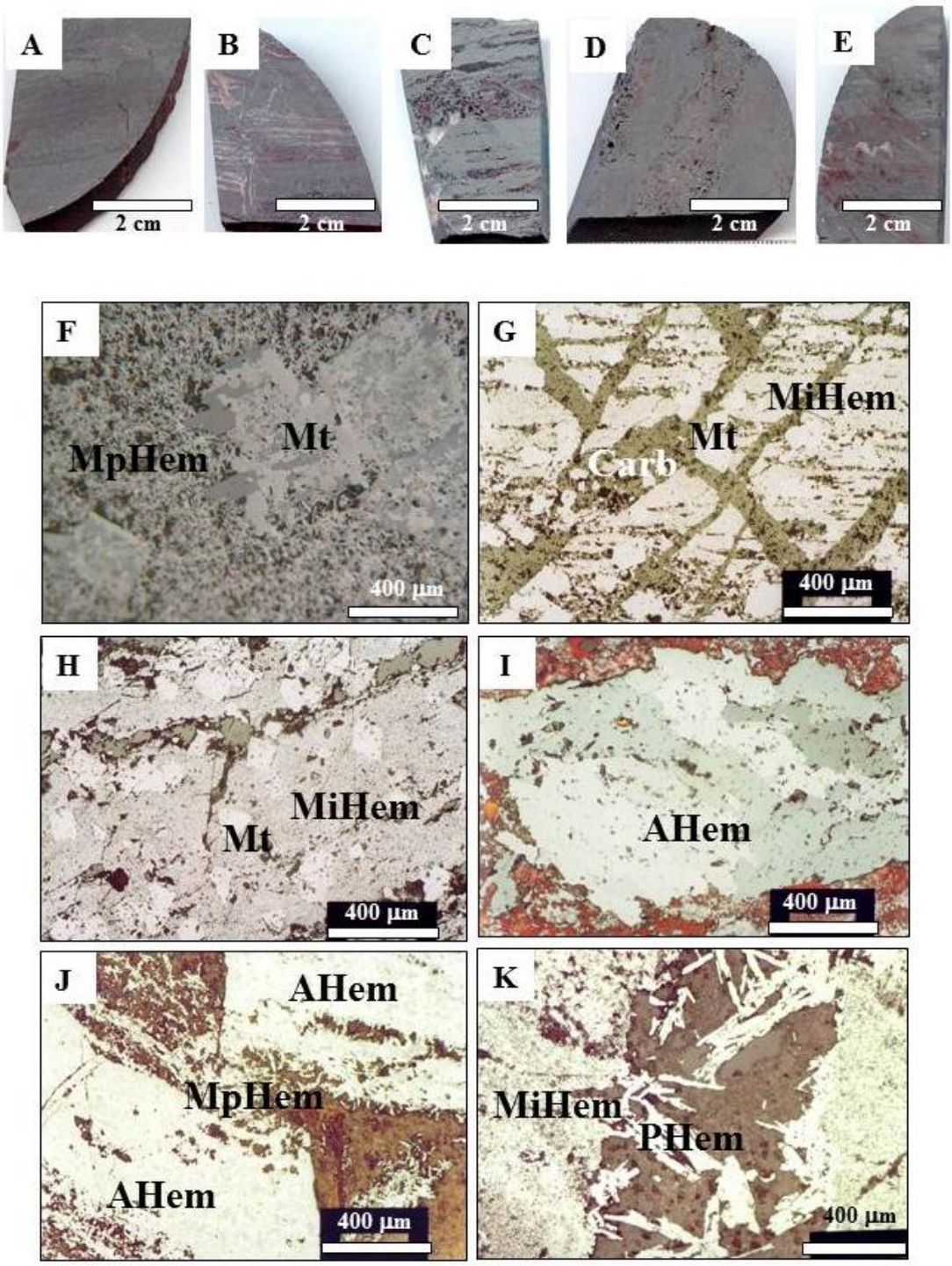

Fig. 7. Main features and characteristics of the different hard ore types. Core samples from A to E and photomicrograph from F to K. A. Hematite-martite ore type from the N4E deposit. B. Carbonate and hematite-martite (banded and brecciated) hard ore from the N4E deposit. C. Martite-hematite (brecciated and quartz veins) hard ore from the N4E deposit. D. Veined hematite (banded and/or brecciated) hard ore from the N5E deposit. E. Hematite and carbonate (brecciated) hard ore from the N5E deposit. F. Martite and MpHem crystals in hematite-martite type, N4E deposit. Note that MpHem grows along martite borders. Reflected light, under crossed polars (50X). G. Carbonate (kutnahorite) veins crosscutting MiHem and Mt bands of carbonate and hematite-martite ore, N4E deposit. Reflected light (50X). H. Mt crystals over MiHem bands in hematite-martite ore association, N4E deposit. Reflected light (50X). I. Anhedral-subhedral hematite portion characterizing brecciated hematite ore, N5E deposit. Reflected light, under crossed polars (50X). J. AHem and MpHem portions in brecciated hematite ore, N5E deposit. Reflected light (50X). K. Platy hematite (PHem)-quartz vein in brecciated ore, N5E deposit. Reflected light (50X). Mineral abbreviations: MiHem = microcrystalline hematite; MpHem = microplaty hematite; Mt = martite; AHem = anhedral hematite.

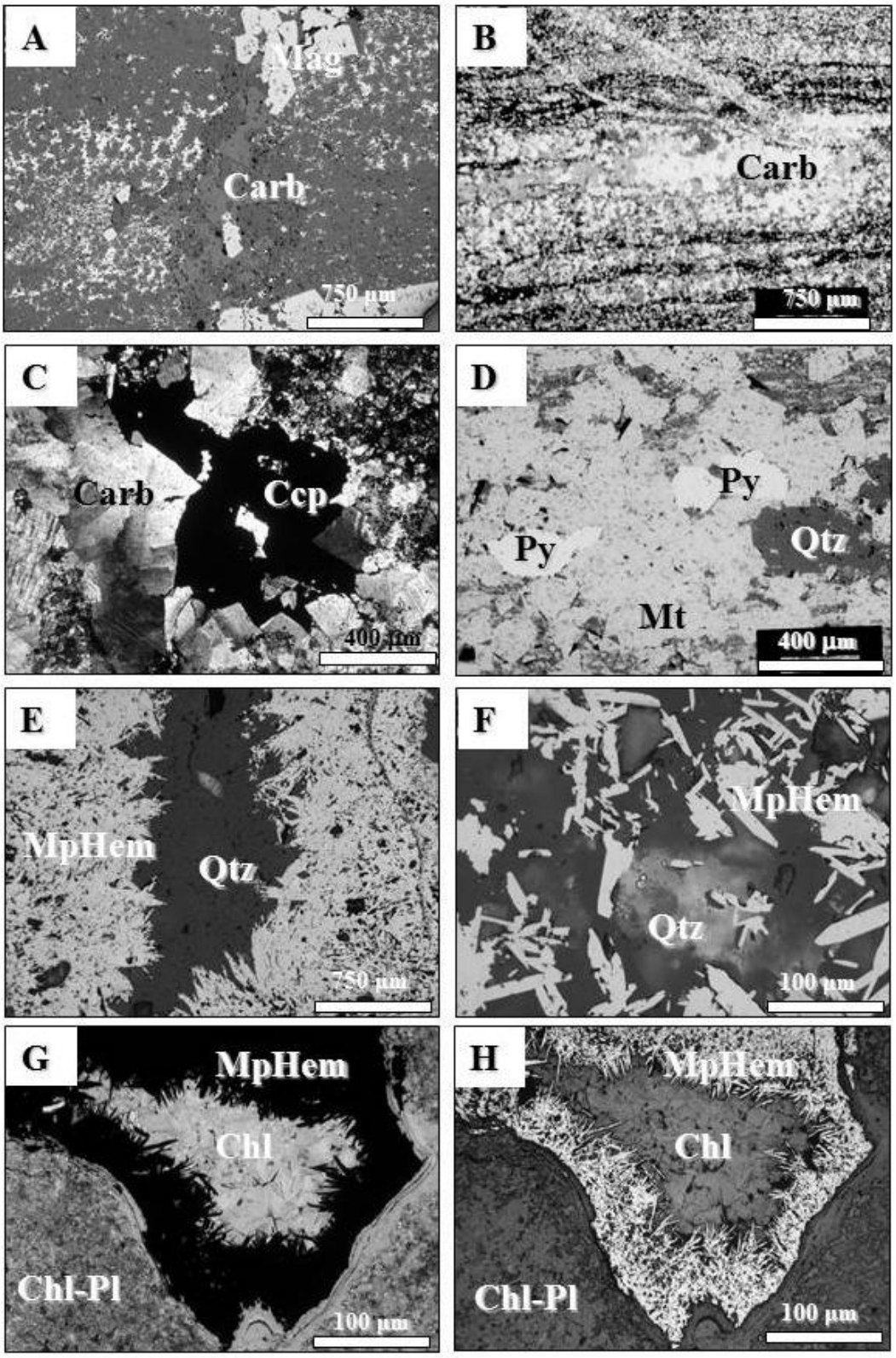

Fig. 8. Photomicrographs displaying some hydrothermal alteration features. A. Magnetite-carbonate (calcite) vein-breccia in altered jaspilite, N4E deposit. Reflected light (25X). B. Carbonate (calcite) vein-veinlets discordant and along jaspilite banding, N4E deposit. Transmitted light, under crossed polars (25X). C. Carbonate (calcite-kutnahorite) and chalcopyrite crystals in brecciated altered jaspilite, N4E deposit. Transmitted light, under crossed polars (50X). D. Pyrite crystals intergrown with martite in altered jaspilite. Reflected light (50X). E. Quartz-microplaty hematite vein, N5S deposit. Reflected light (25X). F. Microplaty hematite intergrown in matrix quartz of hydrothermal breccia from the proximal alteration zone, N4E deposit. Reflected light (200X). G. Chlorite and microplaty hematite replacing amygdale in hydrothermally altered basalt composed by chlorite and plagioclase. Transmitted light, under crossed polars (200X). H. Microplaty hematite replacing amygdale. Reflected light (200X). Mineral abbreviations: Mag= magnetite; Carb= carbonate; Ccp= chalcopyrite; Qtz = quartz; Chl = chlorite; Pl = plagioclase, MpHem = microplaty hematite.

6.1 - Veins and breccias

Detailed logging of about 20 diamond-drill cores, through the N4 and N5 deposits, and petrographic and textural descriptions of veins and breccias were used to establish a vein classification with respect to their location in specific hydrothermal alteration zones and associated iron mineralization and the iron oxide paragenesis (Fig. 9). It must be emphasized that the vein types from the distal alteration zone do not contain hematite, and represent an early mineralization stage. In contrast, hematite is intergrown with quartz, carbonate and sulfides (where present) in veins from the intermediate and proximal alteration zones. Two vein-breccia types characterize the distal alteration zone in jaspilite: V1a – quartz ± sulfide breccias, and V1b – carbonate ± sulfide breccia-veins. The intermediate alteration zone is represented by the following vein types: V2a – quartz ± hematite bedding-discordant veins; V2b - vug-textured quartz + hematite discordant vertical veins; V3 – hematite ± quartz veins crosscut and/or parallel to the jaspilite bedding. The proximal alteration zone is characterized by vein filling in breccia classified as V4 – carbonate-quartz breccia, and V5 – quartz ± microplaty hematite breccia, both are located in high-grade ore.

Quartz is present principally as (i) micro- to cryptocrystalline crystal aggregates of mosaic texture, probably the product of recrystallization of chalcedony and amorphous quartz (Lovering, 1972), (ii) comb-textured crystals observed in V2 and V3 veinlets and veins, and oriented perpendicular to magnetite crystal faces, and (iii) fine to very coarse (8mm), pyramidal crystals that occur along polygonal grain boundaries in V1, V2 and V5 veins.

Carbonate crystals occur in discordant V1 veins or veinlets and/or along jaspilite layers, cementing ore breccias as V4 veins and locally in jasper layers.

The anhedral to euhedral carbonate crystals are generally fine grained, but locally coarse grained (>10 mm). Zoned crystals display a dusty hematite pigment. They are classified as manganese-rich dolomite (i. e., kutnahorite), dolomite and calcite (Figueiredo e Silva, 2004). Calcite is only associated with V1 veins that are concordant and discordant to bedding in jaspilite.

Sulfide minerals: Pyrite is present as fine grained (0.1 to 0.2mm), subhedral and anhedral crystals or grains, and occurs in veins with associated MpHem or along the jaspilite bands. In places, pyrite overgrows kenomagnetite or is intergrown (less commonly included) in martitized magnetite crystals (Fig. 8D). Chalcopyrite crystals are subhedral to euhedral, mainly in textural equilibrium with carbonate (Fig. 8C) or dispersed in anhedral quartz aggregates in V1 veins. Rare chalcopyrite crystals are included in kenomagnetite and locally in jasper bands. Rare covellite is associated with goethite, fine-grained hematite, chalcopyrite, and is found within quartz-rich martite crystals. Locally, veins of native copper and fine-grained gold are observed in jaspilite and martite aggregate, respectively.

Rare very fine monazite crystals were identified using scanning electron microscopy. They are associated with V1 veins.

7. WHOLE-ROCK GEOCHEMISTRY

Major, trace and rare-earth element (REE) analyses of 50 samples from the N1, N4E, N4W, N5E, and N5S deposits include protore jaspilite, hydrothermally altered jaspilite and high-grade iron ore (Figueiredo e Silva, 2004; Lobato *et al.*, 2007; Figueiredo e Silva *et al.*, 2008). Analytical procedures, instruments and standards can be found in Figueiredo e Silva *et al.* (2008). The major-element diagram Fe_2O_3 versus SiO_2 for the N4W, N5E and N5S jaspilites exhibits a negative correlation characterized by the progressive decrease in Fe_2O_3 as SiO_2 increases (Fig. 10A). The Fe_2O_{3Total} contents vary between 48.7 and 63.2 wt percent (34.2 wt % to 44.2 wt % Fe), and SiO_2 contents between 35 and 50 wt percent. Two hydrothermally altered jaspilite samples from the N4W deposit exhibit elevated Fe_2O_3 content of ~ 80 wt percent (c. 60 wt % Fe) similar to the ore samples. The hard ores have a high iron concentration, with N1 samples exhibiting between 68.2 and 69.7 wt percent Fe, and those from N5E between 64 and 67.5 wt percent Fe, with very low SiO_2 contents (Fig. 10A). The Al_2O_3 contents are < 0.3 wt percent in the jaspilites, and < 2 wt percent in the ores; values from 2.3 to 4 wt percent were obtained for high-grade ore samples at the contact with basaltic wall rocks. Trace-element compositions in jaspilites and iron ores are normalized to chondrite (Taylor & McLennan, 1985) (Fig. 10B). The elements Ba, U, Nb and Y are enriched in all types of ores when compared to jaspilites (Fig. 10B). The ores display an enrichment of U on the order of 20 to 200 times compared to jaspilite (Fig. 10B). Ores from the N5E deposit have U values up to 1000 times that of chondrite. The Ba concentration reaches ~ 100 times that of chondrite and 10 times that of jaspilites. The Nb varies up to 10 times chondrite, except in N5E jaspilites where there is no Nb enrichment. The Y contents only exceed chondrite values in ores and hydrothermally altered basaltic rock. Jaspilites and ores from the N5E deposit display depletion of Cu, Zn, Ni (Fig. 10B) and Co, but V is enriched by ~ 20 times chondrite.

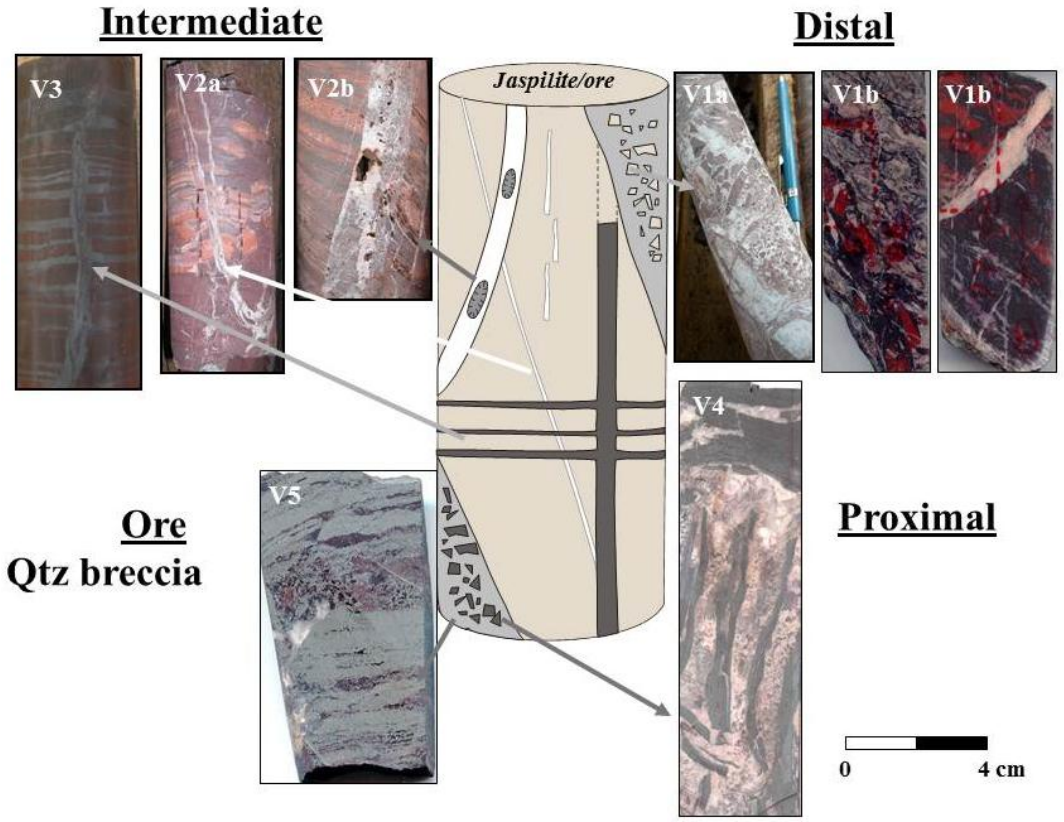

FIG. 9. Schematic diagram illustrating the classification of veins and breccias. Also shown are photographs of examples from core samples. Two vein-breccia types characterize the distal alteration zone in jaspilite: V1a - quartz ± sulfide breccia and V1b - carbonate ± sulfide breccia-veins. The intermediate alteration zone is represented by the following vein types: V2a - quartz ± hematite bedding discordant veins; V2b - vug-textured quartz + hematite discordant vertical veins; V3 - hematite ± quartz veins crosscut and/or along the jaspilite bedding. The proximal alteration zone is characterized by V4 - carbonate (iron cloud)-quartz breccia, and V5 - quartz ± microplaty hematite breccia, both are located in high-grade ore.

The REE data are normalized to chondrite (Nakamura, 1974). The sum of the REE_N in least-altered jaspilites varies in the N4E deposit from 5.6 to 23 ppm, in the N5E deposit from 4.5 to 13.8 ppm, and in the N5S deposit from 4 to 24.9 ppm. In contrast, for the ores this sum is more variable ranging from 6.5 to 14.8 ppm in the N1 deposit, except in two samples, in which ΣREE_N = 103 and 91 ppm, 8.1 to 44.2 ppm for the N4E deposit, and 14.6 to 97 ppm for the N5E deposit. The REE patterns of least-altered jaspilite samples from the N4W, N5E and N5S deposits are shown in Figs. 11A, B and C. Samples from the different deposits exhibit similar fractionation patterns with light REE_N ($LREE_N$) enrichment $(La/Sm)_N$ = 9.53 to 13.69, small to moderated positive Eu anomalies (Eu/Eu* = 1.54 to 2.34), and relatively horizontal patterns for the heavy REE_N ($HREE_N$) that commonly exhibit low contents ($\Sigma HREE_N$ <1 ppm). Samples from N5S display a wider range of REE values, mainly HREE (Fig. 11C).

Ores from the N4E deposit display two different populations (Figs. 11E and F), with higher (14.8 to 44.2 ppm) and lower (8.3 and 8.1 ppm) ΣREE_N. The former displays a LREE enrichment and discrete negative Eu anomaly, whereas the latter, a kutnahorite-bearing ore (Fig. 11F), presents a weakly positive Eu anomaly (1.3 and 1.5).

The characteristic pattern in ores from the N1 deposit, with ΣREE = 11.7 to 14.8 ppm (Fig. 11D), resembles that of the N4W jaspilites (Fig. 11A), except for higher Eu anomalies (2.1 to 2.9) and relative increase in HREE contents. In high-grade, hematite-martite N1 ores, oxides that formed due to the hydrothermal alteration, are microplaty hematite-martite ± tabular hematite; however original MiHem is still preserved. The slightly higher total ΣREE contents of the N1 ores, when compared to N4W jaspilites, may be related to their lack of jasper bands, and also to the larger proportion of newly formed MpHem.

Two distinct chondrite-normalized REE patterns characterize ore samples from N5E deposit. The first (Fig. 11G) shows an almost flat pattern and is characterized by veined hematite ore, locally layered with MiHem, AHem, and THem and MpHem veinlets. The second is represented by two brecciated hematite ore samples and yields the highest ΣREE_N contents, respectively 85.54 and 97.52 ppm (Fig. 11H). They are predominantly comprised of the advanced-stage alteration oxides, with

subhedral to AHem, and also contain tabular, lamellar and euhedral hematite veinlets. This REE pattern shows the most prominent LREE enrichment in comparison to the HREE, a slightly negative Eu anomaly (Eu/Eu* = 0.62 and 0.79), with the possible addition of iron. Michard (1989) related the increase in the concentration of REE, negative Eu anomaly and LREE enrichment to equilibration with low-pH fluids. The ubiquitous presence of newly formed MpHem in these ores suggests a greater incorporation of REE, favored by the same coordination in the structure and size of the ionic radii of REE (Khan *et al.*, 1996), from 1.032 Å (La) to 0.861 Å (Lu) (Grossi Sad & Dutra, 1987).

In comparison to least-altered jaspilites (Figs. 11A, B and C), the N1, N4E and N5E ores yield REE compositional populations progressively enriched in REE, in that order, except for a single N1 sample. In general, there is closer similarity to the HREE than to the LREE chondrite concentrations (Fig. 11D). The $\Sigma LREE_N$ commonly yields higher concentrations, up to 88.2 ppm in N5E ores, and elements with greater standard deviations are represented by Ce, La and Nd, in jaspilites and ores.

Very fine-grained (< 0.01 mm) monazite inclusions in some AHem crystals from N5E deposit were identified under SEM. Their influence on the especially elevated LREE enrichment cannot be discarded.

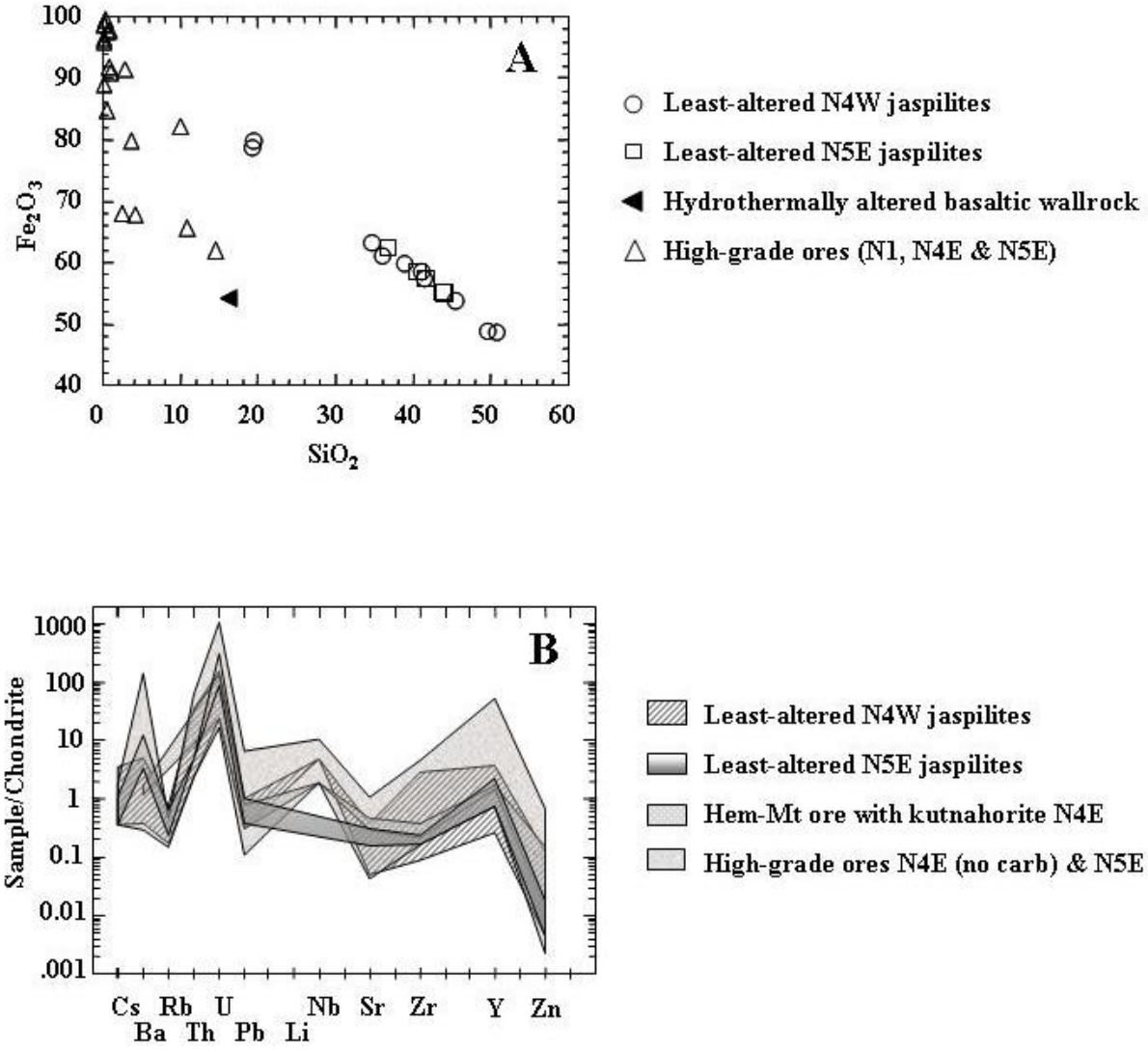

Fig. 10. A. Bivariate plot of Fe2O3 and SiO2 compositions (in wt %) of least-altered jaspilite (here understood as variably altered jaspilite) and high-grade ores from the N4W, N5E and N5Sdeposits. Note negative correlation between Fe2O3 and SiO2 compositional values. Note that two altered jaspilites from the N4W deposit have higher iron contents (~ 80% Fe2O3) than others. B. Trace element distribution in jaspilites and iron ores. Data normalized to chondrite (Taylor and McLennan, 1985).

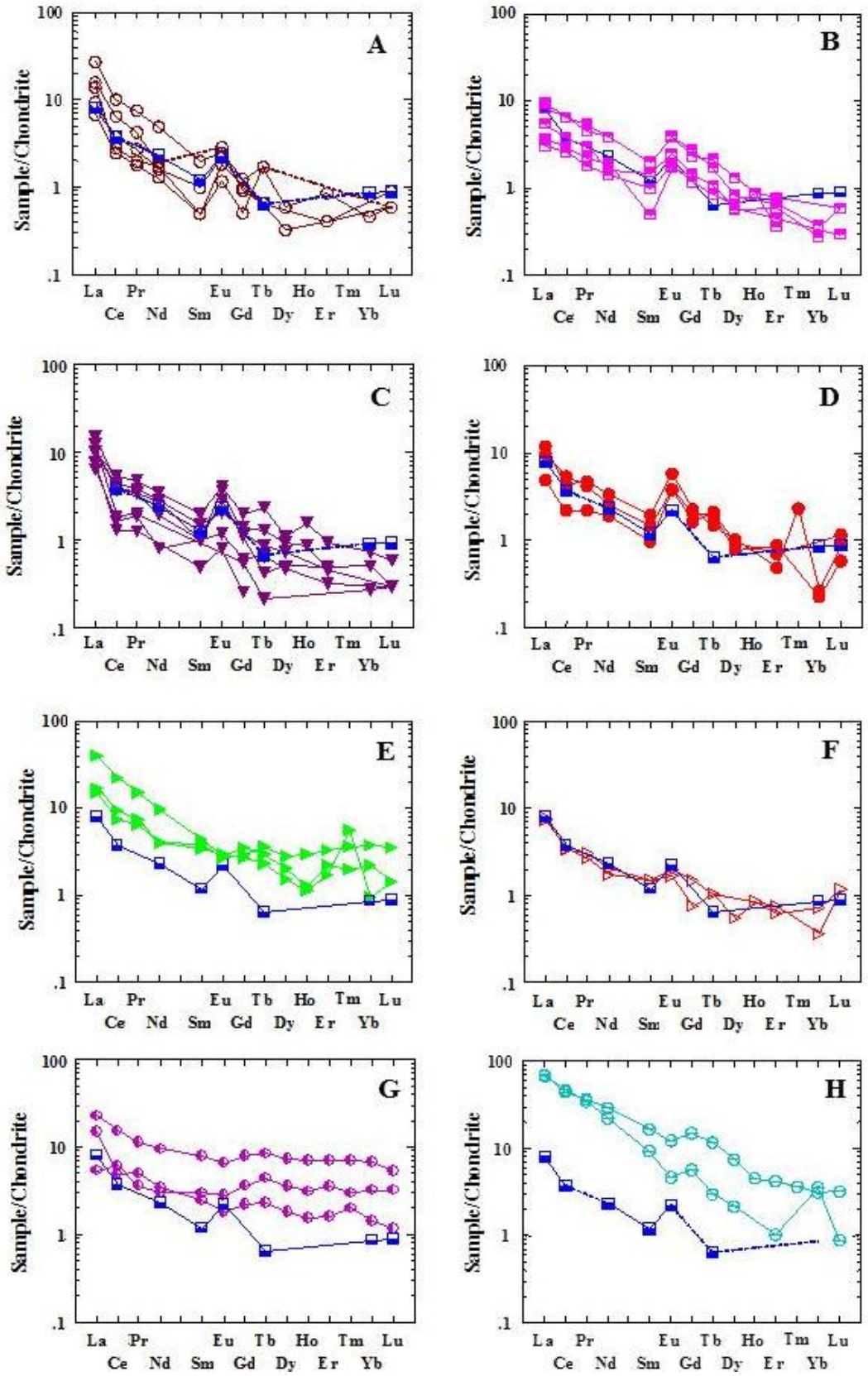

Fig. 11. Chondrite-normalized rare-earth elements plots for the jaspilite and iron ore of the Serra dos Carajás deposit. A. Least to variably altered jaspilites, N4W deposit. B. Least- to variably altered jaspilites, N5E deposit. C. Least to variably altered jaspilites, N5S deposit. D. Hematite-martite ores, N1 deposit. E. Hematite-martite ores, N4E deposit. F. Carbonate (kutnahorite) and hematite-martite ores, N4E deposit. G. Veined hematite ores (locally banded), N5E deposit. H. Brecciated hematite ores with sub- to anhedral hematite, and euhedral-tabular and lamellar hematite veins, N5E deposit. Line with boxes corresponds to average of Isua quartz-magnetite banded iron formation, West Greenland (Dymek and Klein 1988). Data normalized to chondrite (Nakamura 1974).

8. DISCUSSION

8.1 - Review of the genetic models proposed for the Carajás iron ore formation

A number of authors have proposed a hypogene genesis for the iron ore deposits at Carajás, which preceded supergene residual enrichment via leaching of silica (Tolbert et al., 1971; Rezende & Barbosa, 1972; Beisegel et al., 1973; Ladeira & Cordeiro, 1988; Macambira & Lopes, 1996a; Dardenne & Schobbenhaus, 2001; Lindenmayer et al., 2001; Beukes et al., 2002; Klein & Ladeira, 2002; Guedes et al., 2002; Dalstra & Guedes, 2004; Clout & Simonson, 2005). However, no systematic work, either in the public or private domains, existed regarding the hypogene ore, with the exception of a few generalized descriptions (e.g., Dalstra & Guedes, 2004). In addition, there was only restricted information available about the jaspilites at Carajás (e.g. Lindenmayer et al., 2001; Macambira, 2003).

At Carajás a volcanic origin for the so-called "primary iron ore", which contains magnetite, titano-magnetite and ilmenite, was first suggested by Suszczynski (1972), who also mentioned a close association between the hard ore and volcanic rocks. He further suggested that magnetite developed during a magmatic stage, whereas hematite was considered to be post-magmatic. Rezende & Barbosa (1972) and Beisiegel et al. (1973) also proposed a hypogene, metasomatic origin for the massive ore lenses within friable orebodies. Lenses of massive orebodies are associated with intrusive basic dikes, and are located along the hangingwall contact with these dikes, which also crosscut the soft orebodies. Based on these ideas, Melo et al. (1981) suggested that the dikes generated heat for the metasomatic process. The authors also indicated that in the Serra Leste deposits the distribution of the principal lenses of massive hematite ore is structurally controlled.

According to Tolbert et al. (1971), ore formation resulted from leaching of silica from the "iron formations" via weathering due to water percolation that generated residual enrichment of iron oxides and formation of the present orebodies.

Teixeira et al. (1997) first mentioned the occurrence of scarce dolomite lenses at the base of the "BIF". According to the authors, these lenses are relics of former limestone beds that underwent calcite leaching during hydrothermal alteration. These authors indicated that removal of these limestone might have enhanced the "BIF" permeability via fracturing and crack propagation. This would have been followed by silica leaching resulting in iron enrichment of the "BIF". Macambira et al. (1999) pointed out that these carbonate lenses (~ 50 meters wide) represent a "carbonate-bearing jaspilite facies" and suggested that carbonate had been leached from those rocks in order to form hard ores. Due to the local presence of finely laminated dolomite in the N4E deposit, Guedes et al. (2002) and Dalstra & Guedes (2004) defined carbonate-rich protores (45 wt % Fe), which they referred to as "dolomitic iron formation". According to these authors, chert was replaced by dolomite along the layering, accompanied by magnetite development. Dalstra & Guedes (2004) also pointed out that a second dolomitization stage was responsible for carbonate precipitation in veins and vugs, with the local development of breccias. The intense tropical weathering leached the carbonates from "dolomitic iron formation" resulting in the development of friable, soft ore.

Nevertheless, detailed documentation of the hydrothermal alteration stages (Figueiredo e Silva, 2004; Figueiredo e Silva et al., 2008; Lobato et al., 2005a; Zucchetti, 2007) that are spatially and temporally associated with the formation of hard ore have shown that the majority of the carbonate (i.e. dolomite, kutnahorite and calcite) is in the form of discordant and concordant veins and breccias commonly in association with sulfides (e.g. chalcopyrite and pyrite), with or without subordinate magnetite and hematite. Carbonate alteration is only ubiquitous in the N4E and N5E deposits, and is lacking or less common in most other deposits. Moreover, replacement textures of chert or quartz by carbonate are only locally observed. As such, carbonate cannot be considered to be paramount to iron ore formation in the Serra Norte deposits.

8.2 - The REE fingerprint from jaspilite to iron ore

The crystals of magnetite in hydrothermally altered jaspilites are locally surrounded by recrystallized and "clean" jasper, and in equilibrium with fine (~ 0.01mm) vein quartz. In accordance with Taylor *et al.* (2001), the leaching of quartz in BIFs is principally seen as a function of temperature, between 150 to 250º C. This may have been the case in the deposits studied here (Rios *et al.*, 2004; Figueiredo e Silva *et al.*, 2008). The leaching of quartz was accompanied by an increase in martitization of magnetite (Fig. 6D). Quartz and carbonate, therefore, precipitated prior to or synchronous to the formation of magnetite in the jaspilites (Fig. 8A). The leaching of quartz may have been responsible for the general increase in total REE contents, as only magnetite and MiHem remain (Fig. 6C). With the growth of magnetite and MpHem, and the progressive martitization to form AHem, the total REE concentration increased significantly (Figs. 11G and H). This is corroborated by the distribution coefficients K_D of magnetite, which favor the fixation

of LREE (Schock, 1979; Li, 2000). This process may also have favored the relative increase in HREE in the residual hydrothermal fluid, explaining the increase in HREE and the flat REE patterns (Fig. 11) for some ore samples in comparison to least-altered jaspilites. The change in the REE patterns of the ores in relation to jaspilites, encompassing a general REE enrichment with almost flat HREE patterns for some ore samples (Fig. 11G), indicates that the fluids responsible for the early-hydrothermal stage were significantly different or evolved to those of the advanced hydrothermal stage. Indeed, it is during the advanced hydrothermal stages that the EHem and THem generations dominate (Figs. 6F and G).

Hydrothermally altered jaspilites from the N4E, N5E and N5S deposits (Figs. 11A, B and C), ores from N1 and a specific group of samples from the N4E deposit (Figs. 11D to H) display positive Eu anomalies. Locally, N4E and N5E ores have a weakly negative Eu anomaly (Figs. 11E, G and H). According to Grossi & Dutra (1987), no mineral retains Eu^{2+} under accentuated oxidizing conditions, since the element would be unavailable at that oxidation state. However, under reducing conditions, Eu is isolated, potentially being incorporated in the Eu^{2+} state. The initial hydrothermal fluid that interacted with the Serra Norte rocks was relatively reducing (*i.e.* fo_2 in equilibrium with magnetite), probably causing Eu reduction, which may be corroborated by the formation of magnetite after original hematite. The Eu^{2+} was possibly fixed in the structure of minerals, such as dolomites. For example, in the case of the N4E ores, samples with carbonate do in fact display a positive anomaly (Fig. 11F). With the evolution of the hydrothermal fluids, they become relatively more oxidizing, with the remaining Eu^{2+} not incorporated in the rocks, resulting in REE patterns with a weakly negative Eu anomaly, for example in the high-grade ores (Figs. 11G and H).

Ore samples from selected Hamersley deposits show similar features, with less pronounced enrichment in LREE (Lobato *et al.*, 2007). The overall higher REE contents of the Carajás samples compared to the Hamersley ore samples suggest that different fluid sources may have been involved in the origin of the deposits. For Carajás, a magmatic fluid source mixed with meteoric waters has been postulated (Lobato *et al.*, 2005b; Figueiredo e Silva *et al.*, 2007a, 2008), whereas, for example, Hagemann *et al.* (1999) and Thorne *et al.*, (2004) suggest that basinal brines were involved in the origin of the Mt. Tom Price deposit.

9. CONCLUSIONS

The giant Serra Norte Carajás iron ore deposits are hosted by the metavolcano-sedimentary sequence of the Grão Pará Group, Itacaiúnas Supergroup, where the jaspilitic protore and high-grade iron ores (> 64 wt % Fe) are under- and overlain by low metamorphic grade basaltic rocks. The iron ore forming age is considered to be Paleoproterozoic age (Lobato *et al.*, 2005b, 2008; Santos *et al.*, 2010). Detailed mineralogical, geochemical and fluid chemistry investigations on the Serra Norte Carajás iron ore deposits revealed the following:

1. Considering the hydrothermal origin of iron ore forming event at the studied Serra Norte iron ore deposits (Guedes *et al.*, 2002; Figueiredo e Silva, 2009; Lobato *et al.*, 2005b), the sequential order of oxides that follows the original microcrystalline hematite-MiHem is interpreted as: magnetite → martite with or without associated kenomagnetite → microplaty hematite (MpHem) → anhedral hematite (AHem) → euhedral (EHem) and/or tabular hematite (Them). Other mineralogical modifications are: (i) recrystallization and the cleansing of jasper with the formation of chert and fine quartz; (ii) progressive leaching of chert and quartz, leaving oxides and a significant volume of empty spaces as vugs; (iii) silicification and dolomitization with associated sulfides and oxides in veins, breccias and along jaspilite bands; (iv) advanced martitization with the formation of AHem, partial MiHem recrystallization to AHem and partially filling spaces with microplaty/platy hematite; (v) continued space-filling by comb-textured EHem and THem in veinlets and along bands.

2. The iron mineralization involved hydrothermal fluids probably under epizonal conditions. Comb textures defined by quartz, hematite and talc, as well as preserved primary amygdales in basaltic rocks (Zucchetti, 2007) and spherulites in jaspilites, are typical of deposits formed under epizonal conditions and preserved at shallow, low-temperature crustal conditions.

3. Two different populations of REE patterns are notable: (i) those characteristic of the jaspilites, ore samples from the N1 deposit and a group from the N4E deposit, which indicate a distinct LREE enrichment and positive Eu anomalies, similar to patterns displayed by Archean BIFs worldwide; and (ii) those of N5E ores that are almost flat, with relative enrichment in both LREE and HREE. Another group of N5E brecciated hematite ores display high total REE contents, principally LREE, which may reflect the fixation of these elements in hematite.

4. The REE enrichment in ores and the changes in the shapes of the REE patterns indicate a hydrothermal fluid evolution, where silica leaching may have resulted in a relative general REE increase during the early hydrothermal stage. The LREE increase was more accentuated during the

formation of magnetite and MpHem, and the advance of martitization to AHem. This may have favored the relative increase of HREE in the residual fluid, resulting in an increase in HREE in advanced mineralization stage precipitates and almost flat REE patterns. It is during the advanced hydrothermal stages that the generation of euhedral and tabular hematite was dominant. The increase in REE concentrations in N4E and N5E ore samples further suggests the presence of significant amounts of Fe in the mineralizing fluid.

5. The mineralogical, geochemical and isotopic changes of jaspilites and ores attest to a hydrothermal origin for the formation of the hypogene high-grade iron ores, via interaction with: (i) an early-stage, high-salinity, relatively reducing magmatic fluid (Figueiredo e Silva *et al.*, 2008), which leached silica, formed magnetite and precipitated quartz, carbonate and sulfides; (ii) an intermediate stage fluid that evolved to more oxidizing conditions, with the advance of martitization, increase in the REE concentration and precipitation of hematite in quartz veins; (iii) a late hydrothermal fluid of both low and high salinities, associated with the development of euhedral- and/or tabular-hematite bearing veins. The main hydrothermal fluid flow was probably focused along the original jaspilite-basaltic contact (Lobato *et al.*, 2005b) with intensive lateral fluid diffusion through the jaspilitic sequence and less intense diffusion through the basaltic rocks as these had a more isotropic fabric when compared to banded jaspilites. An inherited Archean structural framework prepared the terrane for the iron mineralizing hydrothermal fluids, as the hard orebodies formed mainly in the hinge zone (e.g., the. N5E deposit) of large folds, and associated with splays from existing shear zones (Rosière *et al.*, 2006).

10. ACKNOWLEDGMENTS

The authors wish to acknowledge Vale for their technical, logistic and financial support during our research. Our special thanks to all technicians, helpers and geologists in Carajás who throughout the years made this work possible. Thanks are due to the research staff at the Centre for Exploration Targeting, University of Western Australia and at the Centro de Pesquisas Prof. Manoel Teixeira da Costa, Universidade Federal de Minas Gerais. RCFS thanks Coordenação de Aperfeiçoamento de Pessoal de Nível Superior (CAPES) for scholarships during her Msc and PhD degrees. Finally, we would like to express our appreciation to the reviewers and the editorial staff, especially Matheus Kuchenbecker.

11. REFERENCES

Angerer T & Hagemann S G. 2010. The BIF-Hosted High-Grade Iron Ore Deposits in the Archean Koolyanobbing Greenstone Belt, Western Australia: Structural Control on Synorogenic- and Weathering-Related Magnetite-, Hematite-, and Goethite-rich Iron Ore. Econ. Geol, **105**: 917-945.

Araújo O.J.B. & Maia R.G.N. 1991. Programa levantamentos geológicos básicos do Brasil. Projeto especial mapas de recursos minerais, de solos e de vegetação para a área do Programa Grande Carajás: Subprojeto Recursos Minerais, Serra dos Carajás, Folha SB.22-Z-A. Brasília, DNPM/Companhia de Pesquisa e Recursos Minerais-CPRM, 152 p.

Araújo O.J.B., Maia R.G.N., João X.S.J., Costa J.B.S. 1988. A megaestruturação arqueana da folha Serra dos Carajás: Congresso Latino-Americano de Geologia, 7th, Belém, Anais, 1, p. 324-328.

Avelar V.G., Lafon J.M., Correa Jr. F.C., Macambira E.M.B. 1999. O magmatismo arqueano da região de Tucumã, Província Mineral Carajás, Amazônia Oriental, Brasil: novos dados geocronológicos. *Revista Brasileira de Geociências*, **29**: 453-460.

Barley M.E., Pickard A.L., Hagemann S.G., Folkert S.L. 1999. Hydrothermal origin for the 2 billion year old giant iron ore deposit, Hamersley Province, Western Australia. *Min. Dep.*, **34**: 784-789.

Barros C.E.M. & Barbey P. 1998. A importância da granitogênese tardi-arqueana na evolução tectono-metamórfica da Província Mineral de Carajás. *Revista Brasileira de Geologia*, **28**: 513-522.

Barros C.E.M. & Barbey P. 2000. Significance of garnet-bearing metamorphic rocks in the Archean supracrustal series of the Carajás Mining Province, Northern Brazil. *Revista Brasileira de Geologia*, **30(3):** 367-370.

Barros C.E.M., Barbey P., Boullier A.M. 2001. Role of magma pressure, tectonic stress and crystallization progress in the emplacement of syntectonic granites. The A-type Estrela Granite Complex (Carajás Mineral Province, Brazil). *Tectonophysics*, **343**: 93-109.

Beisiegel V.R., Bernardelli A.L., Drummond N.F., Ruff A.W., Tremaine J.W. 1973. Geologia e recursos minerais da Serra dos Carajás. *Revista Brasileira de Geociências*, **3(4):** 215-242.

Beukes N.J., Gutzmer J., Mukhopadhyay J. 2002. The geology and genesis of high-grade hematite iron ore deposits: Australasian Institute of Mining and Metallurgy, Publication Series **7**: 23-29.

Bizzi L.A., Schobbenhaus C., Gonçalves J.H., Baars F.J., Delgado I.M., Abram M.B., Leão Neto R., de Matos G.M.M., Santos J.O.S. 2001. Geologia, Tectônica e Recursos Minerais do Brasil: Sistema de Informações Geográficas–SIG e Mapas na Escala 1:2 500 000. 4ª Edição, 4 CD-rom. Companhia de Pesquisa e Recursos Minerais-CPRM.

Borges A.W.G. 1994. *Geologia da porção Norte da Jazida de Ferro N4, Carajás-Pará*. Universidade Federal do Pará, Trabalho de Conclusão de Curso, 60 p.

Cabral A.R., Rocha Filho O.G., Jones R.D. 2003. Hydrothermal origin of soft hematite ore in the Quadrilátero Ferrífero of Minas Gerais, Brazil. Petrographic evidence from the Gongo Soco iron ore deposit. *Applied Earth Science*, **112**: 279-286.

Clout J.M.F. & Simonson B.M. 2005. Precambrian iron formations and iron formation-hosted iron ore deposits. *Econ. Geology*, 100th Anniversary Volume, p. 643-679.

Costa L.P. 2007. *Caracterização das seqüências metavulcanossedimentares da porção leste da Província Mineral Carajás, Pará.* Belo Horizonte, Brazil, Universidade Federal de Minas Gerais, Departamento de Geologia, Unpublished M.Sc. dissertation, 113 p.

CVRD 1996. Resumo dos aspectos geológicos da Província Mineral Carajás, in Guia de excursão: DIGEB/DEPAB/ GIMB/SUMIC, p. 392-403.

CVRD 2004. Atualização dos recursos e reservas provadas e prováveis das minas de N4 e N5, in Relatório de pesquisa: Departamento Nacional de Produção Mineral-DNPM, I, 197 p.

CVRD 2007. Form annual report pursuant to section 13 or 15(d) of the securities exchange act of 1934, United States Securities and Exchange Commission.

Dall'Agnoll R. & de Oliveira D.C. 2007. Oxidized, magnetite-series, rapakivi-type granites of Carajás, Brazil: Implications for classification and petrogenesis of A-type granites. *Lithos*, **93(3-4):** 215-233.

Dalstra H.J. & Guedes S. 2004. Giant hydrothermal hematite deposits with Mg-Fe metasomatism: a comparison of the Carajás, Hamersley, and other iron ores. *Econ. Geo.*, **99**: 1793-1800.

Dardenne M.A., Ferreira Filho C.F., Meirelles M.R. 1988. The role of shoshonitic and calc-alkaline suites in the tectonic evolution of the Carajás district, Brazil. *Journal of South Americam Earth Science*, **1(4):** 363-372.

Dardenne M.A. & Schobbenhaus C. 2001. *Metalogênese do Brasil*, Editora Universidade de Brasília, 392 p.

Dias G.S., Macambira M.J.B., Dall'Agnol R., Soares A.D.V., and Barros C.E.M. 1996. Datação de zircões de sill de metagabros: comprovação da idade arqueana da Formação Águas Claras, Carajás-Pará: In: Simpósio de Geologia da Amazônia, 5th, Belém, Brazil, Extended abstract: 376-379.

DOCEGEO 1988. Revisão litoestratigráfica da Província Mineral de Carajás. In: Proceedings of Congresso Brasileiro de Geologia 35th, Sociedade Brasileira de Geologia: Belém, Brazil, p. 11-54.

Domingos F.H.G. 2005. *Geometria, cinemática e história tectônica das rochas da Serra Norte, Carajás-PA.* Belém, Brazil, Universidade Fereral do Pará, Unpublished M.Sc. dissertation, 119 p.

Dymek R.F. & Klein C. 1988. Chemistry, petrology, and origin of banded iron formation lithologies from the 3800 Ma Isua supracrustal belt, West Greenland. *Precambrian Res.*, **39**: 241-302.

Faraco M.T.L., Carvalho J.M.A., Klein E.L. 1996. A carta metalogenética da Província Carajás/Sul do Pará–Folha Araguaia (SB.22). In: Congresso Brasileiro de Geologia, 39, Salvador, Anais, **3**: 248-250.

Figueiredo e Silva R.C. 2009. *Evolução e gênese do minério de ferro hidrotermal nos depósitos da Serra Norte, Província Mineral Carajás*. Belo Horizonte, Brazil, Universidade Federal de Minas Gerais, Departamento de Geologia, Unpublished PhD thesis, 236 p.

Figueiredo e Silva R.C. 2004. *Caracterização petrográfica e geoquímica de jaspilitos e minérios de ferro, Província Mineral Carajás, Pará: implicações para a mineralização de ferro.* Belo Horizonte, Brazil, Universidade Federal de Minas Gerais, Departamento de Geologia, Unpublished M.Sc. dissertation, 151 p.

Figueiredo e Silva R.C. Hagemann S.C., Lobato L.M., Banks D. 2007a. Hydrothermal fluid characteristics and evolution for the giant Carajás North Range iron deposits, Brazil. In: Biennial Conference European Current Research of Fluid Inclusion (ECROFI) 19th. University of Bern, Switzerland, Abstract: 98.

Figueiredo e Silva R.C., Hagemann S.G., Lobato L.M., Venemann T. 2007b. Iron oxide paragenesis, quartz vein chronology and hydrothermal fluid evolution at the giant North Range Carajás iron deposits in Brazil. In: Biennial Meeting of the Society for Geology Applied to Mineral Deposits 9th. Proceedings, SGA, Dublin, Ireland, Extended abstract, **2**: 1223-1226.

Figueiredo e Silva R.C., Lobato L.M., Rosière C.A., Hagemann S.G, Zucchetti M., Baars F.J., Morais R., Andrade I. 2008. Hydrothermal origin for the jaspilite-hosted, giant Serra Norte iron ore deposits in the Carajás mineral province, Para State, Brazil. *In:* Hagemann, S.G., Rosière, C.A., Gutzmer, J., and Beukes, N.J. (eds.), BIF-related high-grade iron mineralization. *Reviews in Econ. Geo.*, **15**: 255-290.

Galarza M.A. & Macambira M.J.B. 2002. Petrologia e geocronologia das rochas encaixantes do depósito de Cu-Au Igarapé Bahia, Província Mineral de Carajás, Pará, Brasil, in Klein, E.L., Vasquez, M.L., Rosa-Costa, L.T. (Eds.), Contribuições à Geologia da Amazônia 3, Belém, SBG, p. 153-168.

Gibbs A.K. & Wirth K.R. 1990. Geologic setting of the Serra dos Carajás iron deposits. *In*: Chauvel, J.-J. et al., editorial board, Ancient Banded Iron Formations (Regional Presentations), Theophrastus Publications, S.A., Athens, Greece, p. 83-102.

Gibbs A.K., Wirth K.R., Hirata W.K., Olszewski Jr. W.J. 1986. Age and composition of the Grão Pará Group volcanics, Serra dos Carajás. *Revista Brasileira de Geociências*, **16(2)**: 201-211.

Grainger C.J., Grooves D.I., Tallarico F.B., Fletcher I.R. 2008. Metallogenesis of the Carajás Mineral Province, Southern Amazon Craton, BVrazil: Varying styles of Archean through Paleoproterozoic to Neoproterozoic base- and precious-metal mineralization. *Ore Geology Reviews*, **33**: 451-484.

Grossi Sad J.M. & Dutra C.V. 1987. Fracionamento dos elementos terras raras e suas aplicações em metalogênese. Parte I: Princípios gerais. In: Congresso Brasileiro de Geoquímica, 1st, Porto Alegre, 40 p.

Guedes S.G. 2000. *Evidências de alteração hidrotermal na formação ferrífera bandada e minérios de ferro de N4, N5 e Serra Leste, Serra dos Carajás-Pará, Brasil.* Belo Horizonte, Brazil, Universidade Federal de Minas Gerais, Departamento de Geologia, Seminário de Qualificação, 61 p.

Guedes S.G., Rosière C.A., Barley M., Lobato L.M. 2002. The importance of carbonate alteration associated with the Carajás high-grade hematite deposits, Brazil. In: Iron Ore 2002 Proceedings, The Australasian Institute of Mining and Metallurgy, Melbourne, Australia, Publication Series **7**: 63-66.

Gutzmer J., Mukhopadhyay J., Beukes N. J., Pack A., Hayashi K., Sharp Z. D. 2006. Oxygen isotope composition of hematite and genesis of high-grade BIF-hosted iron ores In: Memoirs-Geological Society of America 2006, **198**: 257-268.

Hagemann S.G., Barley M.E., Folkert S.L., Yardley B.W., Banks D.A. 1999. A hydrothermal origin for the giant Tom Price iron ore deposit. *In*: Stanley C.J. et al., eds., Mineral deposits: Processes to processing: Rotterdam, Balkema, p. 41-44

Hagemann S.G., Rosière C.A., Lobato L.M., Baars F.J., Zucchetti M., Figueiredo e Silva R.C. 2006. Controversy in genetic models for high-grade BIF related Fe deposits: Unifying or discrete model(s)?. *Applied Earth Science*, Transactions Institute of Mining and Metallurgy B, **115**: 147-151.

Hirata W.K., Rigon J.C., Kadekaru K., Cordeiro A.A.C., Meireles E.M. 1982. Geologia Regional da Província Mineral de Carajás. In: Simpósio de Geologia da Amazônia, Belém, Anais, **1**: 100-108.

Holdsworth R.E. & Pinheiro R.V.L. 2000. The anatomy of shallow-crustal transpressional structures: insights from the Archean Carajás fault zone, Amazon, Brazil. *Journal of Structural Geology*, **22**: 1105-1123.

Huhn S.R.B., Santos A.B.S., Amaral A.F., Ledshan E.J., Gouveia J.L., Martins L.P.B., Montalvão R.G.M., Costa V.G. 1988. O terreno 'granito-greenstone' da região de Rio Maria – sul do Pará. In: Congresso Brasileiro de Geologia, 35th, Belém, Extended abstract: 1438-1452.

Huhn S.R.B., Souza C.I.J., Alburquerque M.C., Leal E.D., Brustolin V. 1999. Descoberta do Depósito Cu(Au) Cristalino: Geologia e Mineralização Associada-Região de Serra do Rabo – Carajás – PA. In: Simpósio de Geologia da Amazônia, 6th, Manaus, Brazil, p. 140-143.

Huhn S.R.B., Soares A.D.V., Medeiros Filho C.A., Magalhães C.C., Guedes S.C., Moura L.G.B., Rego J.L., Cravo C.H. 2000. Carajás Mineral Province, Pará state, north of Brazil. In: International Geological Congress 31st, Rio de Janeiro, Brazil, Field Trip Guide, 24 p.

Khan R.M.K., Sharma S.D., Patil D.J., Naqvi S.M. 1996. Trace, rare-earth element, and oxygen isotopic systematics for the genesis of banded iron-formations: Evidence from Kushtagi schist belt, Archean Dharwar Craton, India. *Geochimica et Cosmochimica Acta*, **60**: 3285-3294.

Klein C. & Ladeira E.A. 2002. Petrography and geochemistry of the least-altered banded iron-formation of the Archean Carajás Formation, northern Brazil. Econ. Geo., **97**: 643-651.

Krymsky R.Sh., Macambira J.B., Macambira M.B.J. 2002. Geocronologia U-Pb em zircão de rochas vulcânicas da Formação Carajás, Estado do Pará. In: Simpósio sobre vulcanismo e ambientes associados, 2nd, Belém, p. 41.

Kullerud G., Donnay G., Donnay J.D.H. 1969. Omission solid solution in magnetite: kenotetrahedral magnetite. *Zeitschrifft der Kristallographie*, **128**: 1-17.

Ladeira E.A. & Cordeiro J.R.C. 1988. Jazida N4E: Reavaliação dos corpos de hematita dura e jaspilitos. In: Proceedings of Congresso Brasileiro de Geologia 35th, Sociedade Brasileira de Geologia: Belém, Brazil, p. 103-120.

Li Y.H. 2000. *A compendium of geochemistry: from solar nebula to the human brain*. Princeton University Press, 475 p.

Lindenmayer Z.G. 1990. *Salobo Sequence, Carajás, Brazil: geology, geochemistry and metamorphism*. London, Canada, University of Western Ontario, Department of Earth Sciences, Unpublished Ph.D. thesis, 406 p.

Lindenmayer Z.G. & Fyfe W.S. 1992. Comparação preliminar entre os metabasaltos dos grupos Parauapebas e Salobo da bacia Carajás, PA. In: Congresso Brasileiro de Geologia, Anais, **2**: 33-34.

Lindenmayer Z.G., Laux J.H., Teixeira J.B.G. 2001. Considerações sobre a origem das formações ferríferas da formação Carajás, Serra dos Carajás. *Revista Brasileira de Geociências*, **31(1):** 21-28.

Lobato L.M., Figueiredo e Silva R.C., Rosière C.A., Zucchetti M., Baars F.J., Seoane J.C.S., Rios F.J., Monteiro, A.M. 2005a. Hydrothermal origin for the iron mineralisation, Carajás Province, Pará State, Brazil. In: Iron Ore 2005 Proceedings, The Australasian Institute of Mining and Metallurgy, Perth, Australia, Publication Series 8, p. 99-110.

Lobato L.M., Rosière C.A., Figueiredo e Silva R.C., Zucchetti M., Baars F.J., Seoane J.C.S., Rios F.J., Pimentel M., Mendes G.E., Monteiro A.M. 2005b. A mineralização hidrotermal de ferro da Província Mineral de Carajás - Controle estrutural e contexto na evolução metalogenética da província. *In*: Marini O.J., de Queiroz E.T., and Ramos B.W., eds., Caracterização de depósitos minerais em distritos mineiros da Amazônia. DNPM/Fundo Setorial Mineral (CT-Mineral/FINEP)/ADIMB, Brasília, Brazil, p. 25-92.

Lobato L.M., Figueiredo e Silva R.C., Hagemann S.G., Thorne W. 2007. Mineralizing fluid evolution and REE patterns for the hydrothermal Carajás iron ores, Brazil, and for selected Hamersley iron deposits, Australi. In: Biennial Meeting of the Society for Geology Applied to Mineral Deposits 9. Proceedings, SGA, Dublin, Extended abstract, **2**: 1227-1230.

Lobato L.M., Hagemann S.G., Figueiredo e Silva R.C., Thorne W., Zucchetti M., Gutzmer J. 2008. Hypogene hydrothermal alteration associated with BIF-related iron ore mineralization. *In*: Hagemann, S.G., Rosière, C.A., Gutzmer, J., and Beukes, N.J., BIF-Related High-Grade Iron Mineralization. *Reviews in Econ. Geo.*, **15**: 107-128.

Lopes P.M.S. 1997. *Mineralogia dos minérios de ferro da jazida N4E, Carajás-PA.* Pará, Brazil, Universidade Federal do Pará, Trabalho de Graduação, 66 p.

Lovering T.G. 1972. *Jasperoid in the United States- its characteristics, origin, and economic significance*. U.S. Geological Survey Professional Paper 710, 164 p.

Macambira J.B. 2003. *O ambiente deposicional da Formação Carajás e uma proposta de modelo evolutivo para a Bacia Grão Pará.* São Paulo, Brazil, Universidade Estadual de Campinas, PhD Thesis, 217 p.

Macambira J.B., & Silva V.F. 1995. Estudo petrológico, mineralógico e caracterização das estruturas sedimentares e diagenéticas preservadas na Formação Carajás, Estado do Pará. In: Boletim Museu Para. Emílio Goeldi, Série Ciência da Terra, **7:** 363-387.

Macambira J.B., Macambira M.J.B., Scheller T., Gomes A.C.B. 1996. Geocronologia Pb/Pb e tipologia de zircões de rochas vulcânicas da Formação Carajás - Pará: Indicador da idade dos BIFs. In: Congresso Brasileiro de Geologia, 39th, Salvador, Extended abstract, p. 516-518.

Macambira J.B., Guedes S., Matias P.H. 1999. *Bif* Carbonático na Formação Carajás: Alteração Hidrotermal ou uma Nova Fácies? In: Simpósio de Geologia da Amazônia, 6th, Manaus, Abstract, p. 563-565.

Macambira J.B. & Schrank A. 2002. Químio-estratigrafia e evolução dos jaspilitos da Formação Carajás (PA). *Revista Brasileira de Geociências*, **32(4):** 567-578.

Macambira M.J.B., Ramos J.F.F., Assis J.F.P., Figueiras A.J.M. 1990. Projeto Serra Norte e Projeto Pojuca. Convênio SEPLAN/DOCEGEO/UFPA/DNPM: Relatório final, 150 p.

Machado N., Lindenmayer Z., Krogh T.E., Lindenmayer D. 1991. U-Pb geochronology of Archean magmatism and basement reactivation in the Carajás área, Amazon shield, Brazil. *Precambrian Res.*, **49**: 329-354.

Meireles E.M., Hirata W.K., Amaral A.F., Medeiros Filho C.A., Gato W.C. 1984. Geologia das folhas Carajás e Rio Verde, Província Mineral de Carajás, Estado do Pará. In: Congresso Brasileiro de Geologia, 33, Rio de Janeiro, Anais, **5**: 2164-2174.

Meirelles M.R. 1986. *Geoquímica e petrologia dos jaspilitos e rochas vulcânicas associadas, Grupo Grão-Pará, Serra dos Carajás, Pará.* Brasília, Brazil, Universidade de Brasília, Unpublished M.Sc. dissertation, 171 p.

Meirelles M.R. & Dardenne M.A. 1991. Vulcanismo basáltico de afinidade shoshonítica em ambiente de arco arqueano, Grupo Grão Pará, Serra dos Carajás, Pará. In: Congresso Brasileiro de Geoquímica, 4th, Extended abstract, p. 131-132.

Melo 1981. Jazida N4E, Geologia e Reservas, Distrito Ferrífero da Serra dos Carajás, Rio de Janeiro, Amazônia Mineração S/A, vol. 4.

Michard A. 1989. Rare earth element systematics in hydrothermal fluids. *Geochimica et Cosmochimica Acta*, **53**: 745-750.

Mougeot R. 1996. *Estude de la limite Archeen-Proterozoique et des mineralizations Au, +/_U associees. Exemples de la region de Jacobina (Etat de Bahia, Bresil) et de Carajás (Etat de Para, Bresil,* University of Montpellier II, Unpublished thesis, 301 p.

Morris R.C. 1985. Genesis of iron ore in banded iron-formation by supergene and supergene-metamorphic - A conceptual model. *In*: Wolff, K.H. (ed.), Handbook of Strata-bound and Stratiform Ore dep, Elsevier, **13:** 73-235.

Nakamura N. 1974. Determination of REE, Ba, Fe, Mg, Na and K in carbonaceous and ordinary chondrites. *Geochimica Cosmochimica Acta*, **38**: 757-775.

Netshiozwi S.T. 2002. *Origin of High-Grade Hematite Ores at Thabazimbi Mine, Limpopo Province, South Africa.* Faculty of Science at the Rand Afrikaans University, Msc Dissertation, 135 p.

Olszewski W.J., Wirth K.R., Gibbs A.K., Gaudette H.E. 1989. The age, origin, and tectonics of the Grao Pará Group and associated rocks, Serra dos Carajás, Brazil: Archean Continental Volcanism and rifting. *Precambrian Res.*, **42**: 229-254.

Pinheiro R.V.L. & Holdsworth R.E. 1997. The structure of the Carajás N-4 ironstone deposit and associated rocks: relationship to Archean strike-slip tectonics and basement reactivation in the Amazon region, Brazil. *Journal of South American Earth Sciences*, **10(3-4):** 305-319.

Pinheiro R.V.L. & Holdsworth R.E. 2000. The Anatomy of shallow – crustal transpressional structures: insights from the Archean Carajás fault zone, Amazon, Brazil. *Journal of Structural Geology*, **22**: 1105-1123.

Pinheiro R.V.L., Nezio J.A., Guedes S.C 2001. A falha Carajás e a estruturação tectônica dos depósitos de ferro da Serra Norte, Carajás (PA). In: Simpósio de Geologia da Amazônia, 7th, Belém, Extended abstract, 11-14.

Rezende N.P. & Barbosa A.L.M. 1972. Relatório de Pesquisa – Distrito Ferrífero Serra dos Carajás, Estado do Pará. Mapas e Seções. Departamento Nacional de Produção Mineral – DNPM & CVRD, **2:** 119 p.

Rios F.J., Lobato L.M., Rosière C.A., Figueiredo e Silva R.C., Souza A.S. 2004. Resultados preliminares do estudo metalogenético do minério hematítico de alto teor do depósito de ferro N5 – Carajás, utilizando microscopia e microtermometria de infravermelho, PA. In: Simpósio Brasileiro de Exploração Mineral, 1st, Ouro Preto, Brazil, ADIMB, CD-ROM.

Rosière C.A. & Chemale Jr. F. 2000. Brazilian formations and their geological setting. *Revista Brasileira de Geociências*, **30(2):** 274-278.

Rosière C.A. & Rios F.J. 2004. The origin of hematite in high-grade iron ores based in infrared microscopy and fluid inclusion studies: the example of the Conceição Deposit, Quadrilátero Ferrífero, Brazil. *Econ. Geol.,* **99**: 611-624.

Rosière C.A., Baars F.J., Seoane J.C.S., Lobato L.M., da Silva L.L., de Souza S.R.C., Mendes G.E. 2006. Structure and iron mineralisation of the Carajás Province. *Applied Earth Science*, Transactions Institute of Mining and Metallurgy B, **115(4):** 126-136.

Rosière C.A., Spier C.A., Rios F.J., Suckau V.E. 2008. The Itabirites from the Quadrilátero Ferrífero and related High-grade Iron Ores: an overview. *In*: Hagemann, S.G., Rosière, C.A., Gutzmer, J., and Beukes, N.J., BIF-Related High-Grade Iron Mineralization. *Reviews in Econ. Geol*., **15**: 223-254.

Santos J.O.S. 2003. Geotectônica dos Escudos das Guianas e Brasil-Central. *In*: Bizzi L.A., Schobbenhaus C., Vidotti R.M., Gonçalves J.H. (eds.), Geologia, Tectônica e Recursos Minerais do Brasil, Companhia de Pesquisa e Recursos Minerais–CPRM, p. 169-226.

Santos J.O.S., Lobato L. M., Figueiredo e Silva R.C., Zucchetti M., Fletcher I.R., McNaughton N.J., Hagemann S.G. 2010. Two Statherian hydrothermal events in the Carajás Province: Evidence from Pb-Pb SHRIMP and Pb-Th SHRIMP datings of hydrothermal anatase and monazite. In: VII SSAGI South American Symposium on Isotope Geology, Brasília, Anais, 2010.

Schock H.H. 1979. Distribution of rare-earth and other trace elements in magnetites. *Chemical Geology*, **26**: 119-133.

Seoane J.C.S., Rosière C.A., Baars F.J., Lobato L.M. 2004. Mapeamento litoestrutural 3-D do Grupo Grão Pará, Província Mineral Carajás, PA. In: Simpósio Brasileiro Exploração Mineral, Simpósio Brasileiro de Exploração Mineral, 1st, Ouro Preto, Brazil, ADIMB, CD-ROM.

Silva G.G., Lima M.I.C., Andrade A.R.F., Issler R.S., Guimarães G. 1974. Geologia das folhas SB-22 Araguaia e parte da SC-22 Tocantins. In: Levantamento de Recursos Minerais, Projeto Radam (Departamento Nacional da Produção Mineral–DNPM e Companhia de Pesquisa e Recursos Minerais–CPRM).

Spier C.A., Barros de Oliveira S.M., Rosière C.A. 2003. Geology and geochemistry of the Águas Claras and Pico Iron Mines, Quadrilátero Ferrífero, Minas Gerais, Brazil. *Min. Dep.*, **38**: 751-774.

Suszczynski E. 1972. A origem vulcânica do minério de ferro primário da Serra dos Carajás – Estado do Pará – Região Amazônica. In: Proceedings of Congresso Brasileiro de Geologia 26th, Sociedade Brasileira de Geologia: Belém, Brazil, p. 103-120.

Tassinari C.C.G., Bettencourt J.S., Geraldes M.C., Macambira M.J.C., Lafon J.M. 2000. The Amazonian Craton.; *In*: Cordani, U.G., Milani, E.J., Thomaz-Filho, A., and Campos, D.A. (eds.), Tectonic Evolution of South America, International Geological Congress, Rio de Janeiro, Brasil, p. 41-99.

Taylor D., Dalstra H.J., Harding A.E., Broadbent G.C., Barley M.E. 2001. Genesis of high-grade hematite orebodies of the Hamersley Province, Western Australia. *Econ. Geol.*, **96**: 837-873.

Taylor S.R. & McLennan S.M. 1985. *The continental crust: its composition and evolution.* Blackwell, 312 p.

Teixeira J.B.G. 1994. *Geochemistry, petrology, and tectonic setting of Archean basaltic and dioritic rocks from the N4 Iron ore deposit, Serra dos Carajás, Pará, Brazil.* Departament of Geoscience, Penn State University, Unpublished Ph.D. thesis, 161 p.

Teixeira J.B.G. & Eggler D.H. 1994. Petrology, geochemistry, and tectonic setting of Archean basaltic and dioritic rocks from the N4 iron ore deposit, Serra dos Carajás, Pará, Brazil. *Acta Geológica Leopoldensia*, **40**: 71-114.

Teixeira J.B.G., Ohmoto H., Eggler D.H. 1997. Elemental and oxygen isotope variations in Archean mafic rocks associated with the banded iron-formation at the N4 iron ore deposit, Carajás, Brazil. *In*: Costa, M.L., and Angélica, R.S. (coords.), Contribuições à Geologia da Amazônia, FINEP/SBG, Brazil, p. 161-203.

Thorne W.S., Hagemann S.G., Barley M.E. 2004. Petrographic and geochemical evidence for hydrothermal evolution of the North deposit, Mt Tom Price, Western Australia. *Min. Dep.,* **39**: 766-783.

Tolbert G.E., Tremaine J.W., Melcher G.C., Gomes C.B. 1971. The recently discovered Serra dos Carajás iron ore deposits, Northen Brazil. *Econ. Geol.*, **7:** 985-994.

Tolbert G.E., Tremaine J.W., Melcher G.C., Gomes C.B.. 1973. Genesis of Precambrian iron and manganese deposits. In: Proceedings of the Kiev Symposium, Earth sciences, **9:** 271-280.

Trendall A.F., Basei M.A.S., Laeter J.R., Nelson D.R. 1998. Shrimp zircon U-Pb constraints on the age of the Carajás Formation, Grão Pará Group, Amazon Craton. *Journal of South American Earth Sciences*, **11(3):** 265-277.

UNESCO 1973. Genesis of Precambrian iron and manganese deposits. In: Proceedings of the Kiev Symposium, Earth sciences, **9:** 382 p.

Varajão C.A.C., Bruand A., Ramanaidou E.R., Gilkes R. 2002. Microporosity of BIF hosted hematite ore, Iron Quadrangle, Brazil. In: Anais da Academia Brasileira de Ciências, **74(1):** 113-126.

Zucchetti M. 2007. *Rochas máficas do Supergrupo Grão Pará e sua relação com a mineralização de ferro dos depósitos N4 e N5, Carajás, (PA).*Belo Horizonte, Brazil, Universidade Federal de Minas Gerais, Departamento de Geologia, Unpublished Ph.D. thesis, 125 p.

Zucchetti M. & Lobato, L.M. 2004. Alteração hidrotermal a hematita das rochas máficas associadas aos depósitos de ferro N4 e N5, Província Mineral de Carajás, PA. In: Simpósio Brasileiro de Exploração Mineral, 1st, Ouro Preto, Brazil, ADIMB, CD-ROM.

Zucchetti M., Lobato L.M., Hagemann S.G. 2007. Hydrothermal alteration of basalts that host to the giant Northern Range Carajás iron ore deposits, Brazil. In: Meeting of the Society for Geology Applied to Mineral Deposits 9th, Proceedings, SGA, Dublin, Ireland, Extended abstract, **2**: 1231-1234.

Wirth K.R., Gibbs A.K., Olszewski W.J. 1986. U-Pb ages of zircons from the Grão-Pará Group and Serra dos Carajás Granite, Pará, Brazil. *Revista Brasileira de Geociências*, **16(2):** 195-200.